Available online at www.sciencedirect.com
SCIENCE DIRECT
Biochimica et Biophysica Acta 1741 (2005) 4 – 10
BIOCHIMICA ET BIOPHYSICA ACTA
BBA
http://www.elsevier.com/locate/bba

Rapid report

JNK and PI3k/Akt signaling pathways are required for establishing persistent SARS-CoV infection in Vero E6 cells

Tetsuya Mizutani*[,1], Shuetsu Fukushi[1], Masayuki Saijo, Ichiro Kurane, Shigeru Morikawa

Special Pathogens Laboratory, Department of Virology 1, National Institute of Infectious Diseases, Gakuen 4-7-1, Musashimurayama, Tokyo 208-0011, Japan

Received 2 March 2005; received in revised form 19 April 2005; accepted 20 April 2005
Available online 13 May 2005

Abstract

Persistence was established after most of the SARS-CoV-infected Vero E6 cells died. RNA of the defective interfering virus was not observed in the persistently infected cells by Northern blot analysis. SARS-CoV diluted to 2 PFU failed to establish persistence, suggesting that some particular viruses in the seed virus did not induce persistent infection. Interestingly, a viral receptor, angiotensin converting enzyme (ACE)-2, was down-regulated in persistently infected cells. G418-selected clones established from parent Vero E6 cells, which were transfected with a plasmid containing the neomycin resistance gene, were infected with SARS-CoV, resulting in a potential cell population capable of persistence in Vero E6 cells. Our previous studies demonstrated that signaling pathways of extracellular signal-related kinase (ERK1/2), c-*Jun* N-terminal protein kinase (JNK), p38 mitogen-activated protein kinase (MAPK), and phosphatidylinositol 3′-kinase (PI3K)/Akt were activated in SARS-CoV-infected Vero E6 cells. Previous studies also showed that the activation of p38 MAPK by viral infection-induced apoptosis, and a weak activation of Akt was not sufficient to protect from apoptosis. In the present study, we showed that the inhibitors of JNK and PI3K/Akt inhibited the establishment of persistence, but those of MAPK/ERK kinase (MEK; as an inhibitor for ERK1/2) and p38 MAPK did not. These results indicated that two signaling pathways of JNK and PI3K/Akt were important for the establishment of persistence in Vero E6 cells.

Keywords: SARS-CoV; Persistent infection; c-*Jun* N-terminal protein kinase; Phosphatidylinositol 3′-kinase/Akt

Severe acute respiratory syndrome (SARS) is a newly found infectious disease caused by a novel coronavirus, SARS coronavirus (SARS-CoV) [11,17]. SARS spread from Guangdong Province in China to more than 30 countries in late 2002, causing severe outbreaks of atypical pneumonia. SARS-CoV is an enveloped, single-stranded positive-sense RNA virus with an RNA genome of approximately 30,000 nucleotides encoding at least 15 open reading frames [11]. As the viral virulence and mortality rate of the patients are very high, understanding the mechanisms of the pathogenicity of SARS-CoV is important for the prevention of SARS.

The gene organization of SARS-CoV is similar to those of other coronaviruses. Coronaviruses exhibit a unique ability to establish persistent infections in vivo and in vitro. Mouse hepatitis virus (MHV), a prototype coronavirus, causes central nervous system diseases in rodents. Astrocytes are the predominant cells that harbor persistent viruses in the central nervous system (CNS) [16]. A previous in vitro study also indicated that the astrocytoma cell line DBT has a potential to establish persistent infection after MHV infection [10]. However, the mechanism of establishment of coronavirus persistence has not been yet well understood. Recently, the down-regulation of the pro-apoptotic protein BNip-3 was found in MHV-infected DBT cells by DNA microarray methodologies [2]. In MHV-infected cells, BNip3 levels were significantly decreased at the transcriptional level, and this down-regulation was mediated by the fusion between the viral envelope and the cell membrane. This observation suggested that the anti-apoptotic effect by the down-regulation of BNip3 in MHV-infected DBT cells allows persistent infection.

* Corresponding author. Tel.: +81 42 561 0771; fax: +81 42 564 4881.
E-mail address: tmizutan@nih.go.jp (T. Mizutani).
[1] These authors contributed equally to this work.

0925-4439/$ - see front matter © 2005 Elsevier B.V. All rights reserved.
doi:10.1016/j.bbadis.2005.04.004

Recently, a human intestinal cell line, LoVo cells, was shown to permit SARS-CoV infection, resulting in the establishment of persistent infection [4]. However, the mechanism of persistence in LoVo cell is still unclear. The monkey kidney cell line, Vero E6, is widely used in the SARS-CoV research because of a high sensitivity to the virus infection. Vero E6 cells express a viral receptor, angiotensin converting enzyme (ACE)-2 [9], at high levels, and SARS-CoV infection of Vero E6 causes cytopathic effects after 24 h [13]. We showed that SARS-CoV infection of Vero E6 cells induced apoptosis via caspase-3 [13]. Several signaling pathways are activated in SARS-CoV-infected Vero E6 cells. One of the mitogen-activated protein kinases (MAPKs), p38, was shown to be phosphorylated and to have pro-apoptotic roles, including tyrosine dephosphorylation of signal transducer and activator of transcription (STAT) 3 [13,15]. Although Akt, which is known to act as an anti-apoptosis factor, was also phosphorylated in virus-infected cells, the activity of Akt is not enough to prevent apoptosis in the SARS-CoV-infected cells [14].

In the present study, Vero E6 cells were subcultured routinely in 75-cm^3 flasks in Dulbecco's modified Eagle's medium (DMEM, Sigma, St. Louis, MO, USA) supplemented with 0.2 mM L-glutamine, 100 units/ml penicillin, 100 μg/ml streptomycin, and 5% (v/v) fetal bovine serum (FBS) and maintained at 37 °C in an atmosphere of 5% CO_2. For use in the experiments, the cells were split once they reached 90% confluence and were seeded onto 24-well tissue culture plate inserts or 25-cm^3 (T-25) flasks. The 100% confluent cells were used in the present and previous studies [13–15]. The culture medium was changed to 2% FBS containing DMEM prior to virus infection. We used a SARS-CoV isolate, Frankfurt 1, kindly provided by Dr. J. Ziebuhr.

Our recent studies indicated that SARS-CoV induces apoptosis in Vero E6 cells after 24-h post infection (h.p.i.) [13]. Although almost all of the virus-infected cells showed morphological changes indicative of cell death until 48 h.p.i., very few surviving cells were observed, and these cells grew and formed colonies on 4 days p.i. (d.p.i.). To investigate whether SARS-CoV replicates in these surviving cells, indirect immunofluorescence (IF) staining was performed to detect intracellular viral antigens. As shown in Fig. 1, all the cells showed viral antigens in the cytoplasm at 10 d.p.i. The persistently infected cell culture at 7 passages produced infectious viral particles at 1.26×10^5 PFU/ml. These results indicated that the persistently infected Vero E6 cells produce infectious viruses.

Persistent infection of many RNA viruses in cell culture has been studied. In these studies, it has been demonstrated that the establishment of RNA virus persistent infection in a cell culture is often involved in the generation of defective interfering (DI) particles and reduction of interferons. In the case of measles virus, persistent viral infected Vero cells produced DI particles [3]. Non-

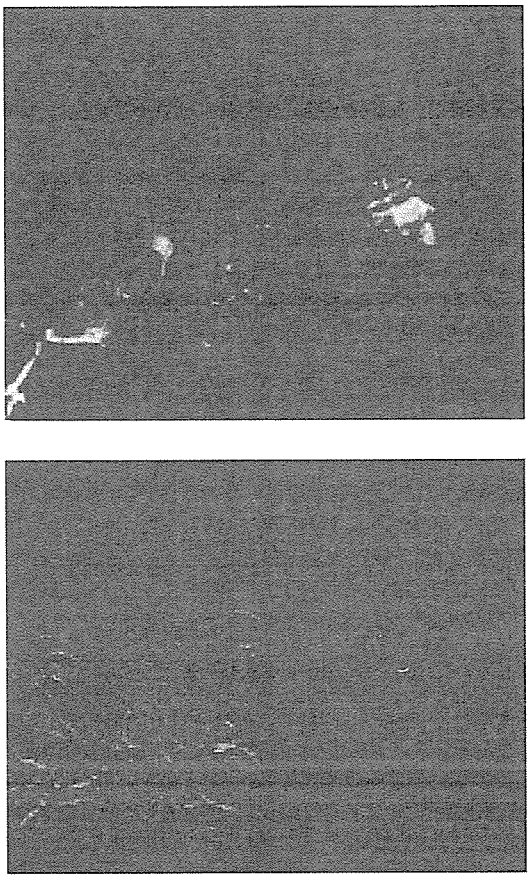

Fig. 1. Indirect immunofluorescence staining of SARS-CoV proteins. For the establishment of persistent infection, the virus was infected to Vero E6 cells at 10 m.o.i. At 10 days p.i., intracellular viral antigens were detected by indirect immunofluorescence staining using rabbit anti-SARS-CoV antibody, which recognizes SARS-CoV proteins (unpublished data). Briefly, cells were spotted onto a 12-well Teflon-coated slideglass, air dried in a biosafety cabinet under UV irradiation, and fixed with 100% pre-chilled acetone. Aliquots of 25 μl of 1:160 diluted anti-SARS-CoV antibody were placed on the coated wells and incubated at 37 °C for 30 min in a moist chamber. After washing with PBS, a fluorescein isothiocyanate (FITC)-conjugated goat anti-rabbit IgG antibody was added at a dilution of 1:40, and incubated for 30 min at 37 °C.

cytopathic (ncp) bovine viral diarrhea virus (BVDV) does not induce type I interferon (IFN), whereas cytopathic (cp) BVDV is able to induce type I IFN [1,6], suggesting that the different capabilities of cp and ncpBVDV to establish persistent infections relates to the difference in their ability to induce IFN [1]. Because Vero E6 cells are known to lack type I interferon genes [5], the involvement of interferon was unlikely in the establishment of SARS-CoV persistence in Vero E6 cells. To investigate whether DI RNAs exist in the persistent cells, Northern blot analysis was performed using a probe complementary to mRNA9 for detecting virus standard genome and all (m)RNAs of SARS-CoV. As shown in Fig. 2, we could not detect any signals of additional viral mRNA in the viral persistent cells at 11 days p.i. This result suggested that the DI virus was not involved in the establishment of persistence in the case of SARS-CoV. However, we cannot

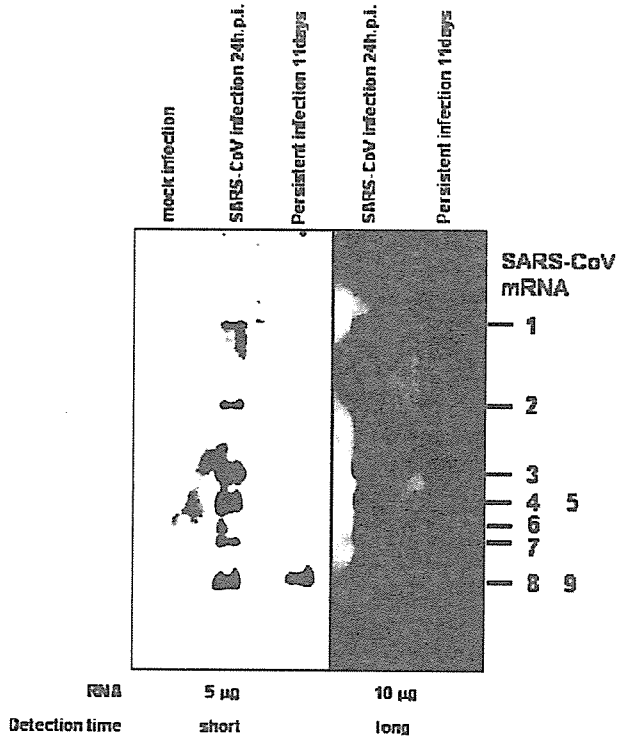

Fig. 2. Northern blot analysis of viral mRNAs. Vero E6 cells were inoculated with SARS-CoV at 10 m.o.i. Total RNA was extracted with Isogen (Nippon Gene, Tokyo, Japan) from SARS-CoV-infected cells at 24 h and 11 days p.i. and from mock-infected cells. RNAs were electrophoresed on 1% agarose gels in the presence of formaldehyde, blotted onto the nitrocellulose membrane. The probe was constructed based on the PCR product of mRNA9. Briefly, viral RNA was reverse-transcribed using SuperScriptIII (Invitrogen, Carlsbad, CA, USA) and the reverse primer, 5′-AGTCAGTCTAATACGACTCACTATAGGGTCCTAAGAAGCTAT-TAAAATTAGC-3′ (29,687 to 29,721 nt of GenBank accession numberNC_004718). The underline indicates the promoter sequence of T7 RNA polymerase. PCR amplification was performed using High Fidelity Platinum Taq DNA polymerase (Invitrogen) using the reverse primer and forward primer, 5′-TGGCTAGCGGAGGTGGTGAAACTGCCC-3′ (28,751 to 28,777 nt). The RNA probe was transcribed from the PCR product using T7 RNA polymerase (Ambion, Austin, TX, USA) under incorporating digoxigenin (DIG RNA labeling kit, Boehringer Mannheim GmbH, Mannheim, Germany). Hybridization and wash were performed as described previously [12]. Left and right panels indicated short and long detection times using the LAS-3000 mini system (Fuji Photo Film Co. Ltd, Tokyo, Japan), respectively.

rule out a possibility that a small amount of DI RNAs appeared in the persistent cells. We measured the densities of mRNA8, 9 and 4, 5 using the LAS-3000 mini system (Fuji Photo Film Co. Ltd, Tokyo, Japan). The amount of mRNA8 and 9 of the persistent cells are 81.4% of the acute infected cells. On the other hand, mRNA4 and 5 of the persistent cells were 12.29% of acute infected cells. In addition, a new round of infection did not induce cell death into persistent infected cells (data not shown). Therefore, we investigated whether persistent cells express a functional SARS-CoV receptor, ACE-2. On Western blotting analysis, ACE-2 was not detected in the persistent cell line (Fig. 3). Interestingly, ACE-2 was also decreased in the acute infection of SARS-CoV. This result suggested that virus particles produced by persistently infected cells could not infect other cells due to a lack of the receptor.

We were interested in determining whether the virus or the host cell is responsible for the establishment of persistent SARS-CoV infection. As shown above, small numbers of Vero E6 cells survived and then continued to grow after SARS-CoV infection. These cells were infected and produced cytopathic viruses (data not shown). The majority of the virus in a seed could induce the apoptotic cell death of Vero E6 cells [13]. If some species of the seed SARS-CoV are involved in an establishment of persistence, seed virus with a limited dilution should not permit persistent infection. The seed SARS-CoV in the present study contained 2×10^8 plaque forming unit (PFU)/ml on Vero E6 cells. The seed virus was diluted from 2×10^2 to 2×10^{-1} PFU, and these virus suspensions were used to inoculate aliquots of 1.5×10^5 cells in T-25 flasks. As shown in Fig. 4, no cell death was observed in cells infected with virus at a dilution of 2×10^{-1} PFU, indicating that viral dilution had been performed correctly. We found that 2×10^0 (=2) PFU-infected cells had fewer plaques than did the 2×10^2 (=200) PFU-infected cells at 36 h.p.i. However, all flasks other than those infected at 2×10^{-1} PFU showed death of almost all cells at 4 d.p.i. and surviving colonies at 7 d.p.i. These colonies became larger at 13 d.p.i. From these results, it seems most likely that some particular viruses in the seed virus did not induce persistent infection.

If a certain Vero E6 cell has the ability to establish persistence after viral infection, such a cell should survive without cell death following infection. To address this possibility, clones from parent Vero E6 cells were established by geneticin-selection (500 μg/ml) after the transfection of pcDNA3 (Invitrogen). Although a total of 115 clones was obtained, 24 clones showed morphological changes or grew very slowly. Therefore, 91 clones that showed similar growth rates in 24-well plates were infected with SARS-CoV at 10 m.o.i. The parental Vero E6 cells

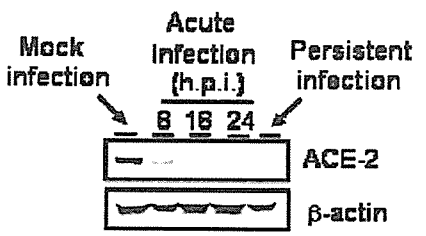

Fig. 3. Down-regulation of ACE-2 by SARS-CoV infection. Western blot of acute infection (8, 18, and 24 h.p.i.) and persistent infection (passage 7) were performed using anti-ACE-2 antibody. Whole-cell extracts were electrophoresed in 10–20% gradient polyacrylamide gel and transferred onto PVDF membranes (Immobilon-P, Millipore, Bedford, MA, USA). We applied two sets of samples to the polyacrylamide gels, and the blots were divided into two sheets for detection by a ProtoBlot II AP system (Promega Co., Madison, WI, USA), as described previously [13–15]. Mouse anti-human ACE-2 ectodomain monoclonal antibody was purchased from R and D systems Inc (Minneapolis, MN, USA) and used at a dilution of 1:1000. Mouse anti-beta actin antibody was purchased from Sigma (St. Louis, MO, USA) and used at a dilution of 1:5000.

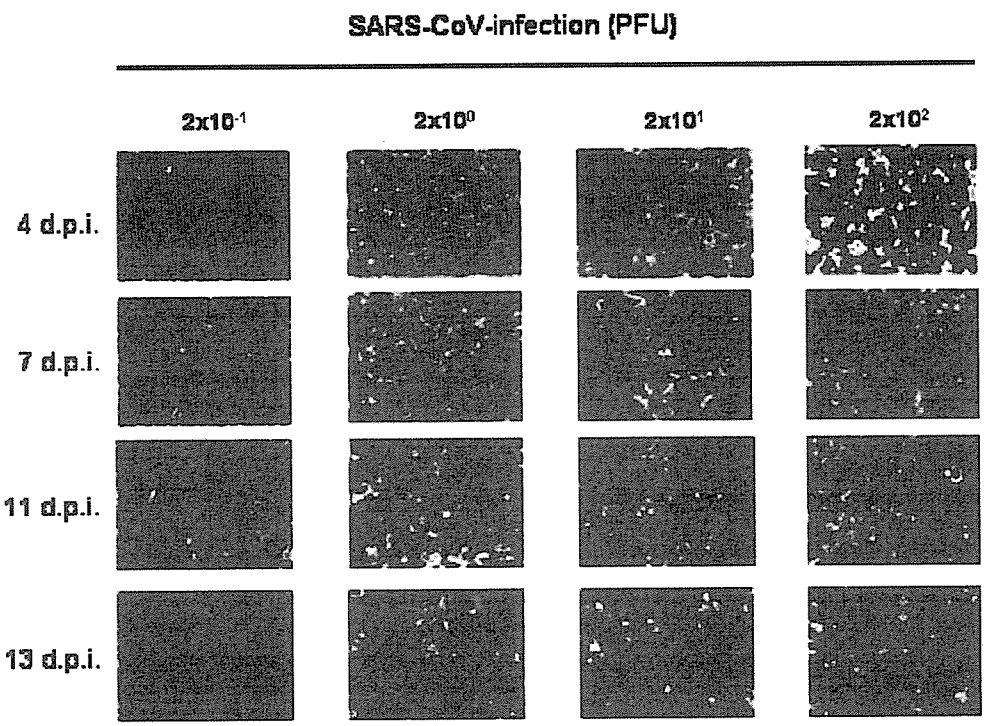

Fig. 4. Establishment of persistent SARS-CoV-infected cells by diluted viruses. Aliquots of 1.5×10^5 Vero E6 cells were inoculated with 2×10^{-1}, 2×10^0, 2×10^1, and 2×10^2 PFU of SARS-CoV. The cells were stained with 0.05% crystal violet after fixing with 20% formaldehyde.

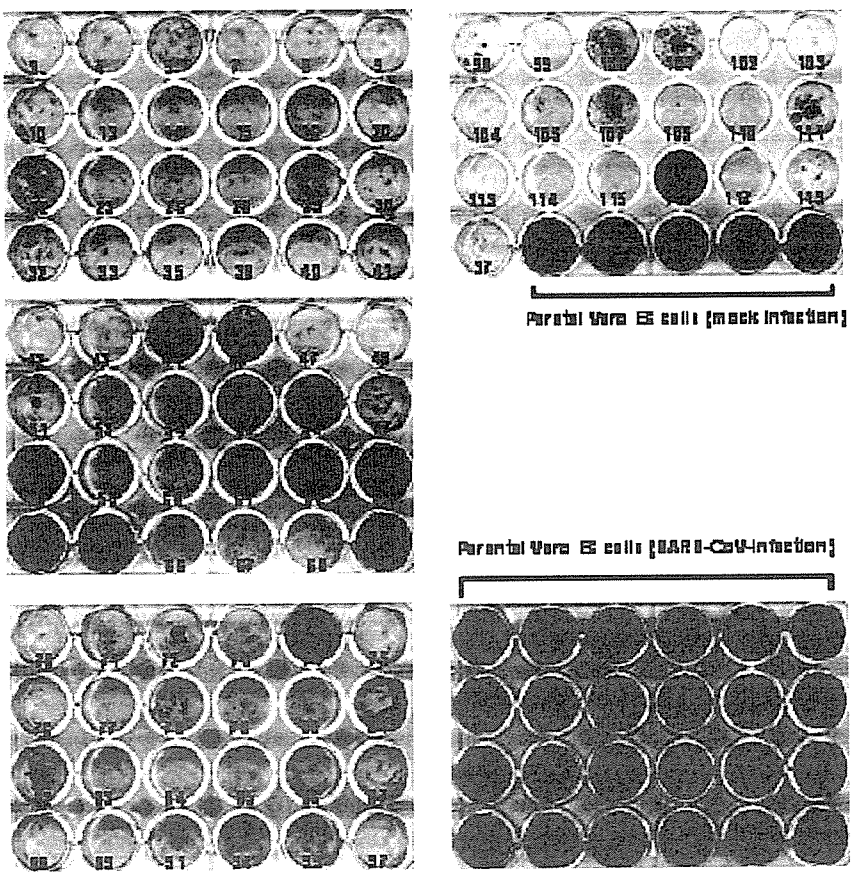

Fig. 5. Persistent SARS-CoV infection of cloned Vero E6 cells. A plasmid, pcDNA3, was transfected into Vero E6 cells using FuGene6 (Roche Diagnostics, Penzberg, Germany), and cloned cells were picked after neomycin selection (500 μg/ml). The 91 cloned cells were inoculated with SARS-CoV at 10 m.o.i. At 20 days p.i., the 24-well plates were fixed and stained.

were used as a control. As shown in Fig. 5, 16 of the 91 clones established persistent infection at 20 d.p.i. Especially, the growth rate of persistently infected clone number 65 was higher than those of the other 15 persistently infected clones. Thus, growth rate was different among the persistently infected clones. This may be due to a difference in a number of survived cells among these 16 cell clones. Interestingly, 75 of the 91 clones failed to establish persistent infection. These results suggested that parental Vero E6 cells always produce a minor population of cells with a potential to allow persistence.

Recently, we reported that extracellular signal-related kinase (ERK1/2), c-*Jun* N-terminal protein kinase (JNK), p38 MAPK, and Akt are phosphorylated in SARS-CoV-infected Vero E6 cells and that viral replication was not affected by the activation of signaling pathways [13–15]. To clarify the signaling pathway important for establishing persistent infection, Vero E6 cells were pre-treated with several concentrations of inhibitors of MAPKs and PI3K/Akt, and then infected with 2 m.o.i. of SARS-CoV. As shown in Fig. 6, SB203580 as an inhibitor of p38 MAPK and PD98059 as an inhibitor of MEK1/2 did not affect the establishment of persistent infection, whereas no surviving cells were observed following treatment with SP600125, an inhibitor of JNK, or LY294002, an inhibitor of PI3K/Akt. This result suggested that JNK and PI3K/Akt are necessary to establish persistence. Our previous study and Fig. 7A indicated that virus-induced Akt phosphorylation was not strong, and it was significantly down-regulated at 24 h.p.i.[14] Therefore, we concluded that the weak Akt activation was not sufficient to protect the viral infected Vero E6 cells from apoptosis. To confirm that the phosphorylation of Akt is necessary to establish persistence, SARS-CoV was infected to clone cell lines of Vero E6, which were showed in Fig. 5. At 20 h.p.i, phosphorylated Akt was not detected in viral infected clone cell lines 43, 48, and 80, which could not establish persistence in Fig. 5, while phosphorylated Akt was detected in viral

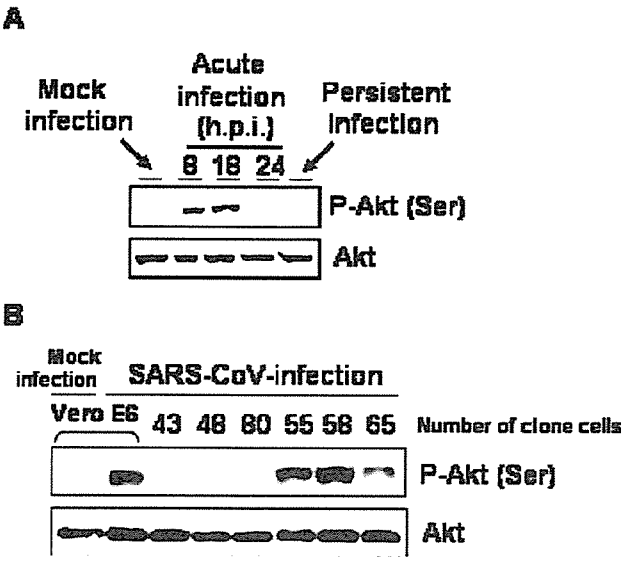

Fig. 7. Phosphorylation status of Akt in viral infected cells. Western blot of acute infection (8, 18, and 24 h.p.i.) and persistent infection (passage 7) were performed using anti-phospho Akt antibody. The rabbit anti-phospho Akt (Ser473) antibody was purchased from Cell Signaling Technology Inc. and used at a dilution of 1:1000. SARS-CoV was infected to cloned Vero E6 cells at 10 m.o.i. The Western blot of the protein samples at 20 h.p.i. was performed using anti-phospho Akt antibody.

infected parental Vero E6, clone cell lines 55, 58, and 65 (Fig. 7B). This result suggested that, at least, the phosphorylation of Akt in viral infected cells were necessary to establish persistence. However, Akt was not phosphorylated in persistent cell lines (Fig. 7A). The phosphorylation of Akt may not be necessary to maintain persistence after establishment.

The present study showed that Vero E6 cells persistently infected with SARS-CoV were established and maintained after multiple passages. A population of cells produced from parental Vero E6 cells may have the potential to support persistent infection. The present study also showed that JNK or PI3K/Akt activation during SARS-CoV infection was

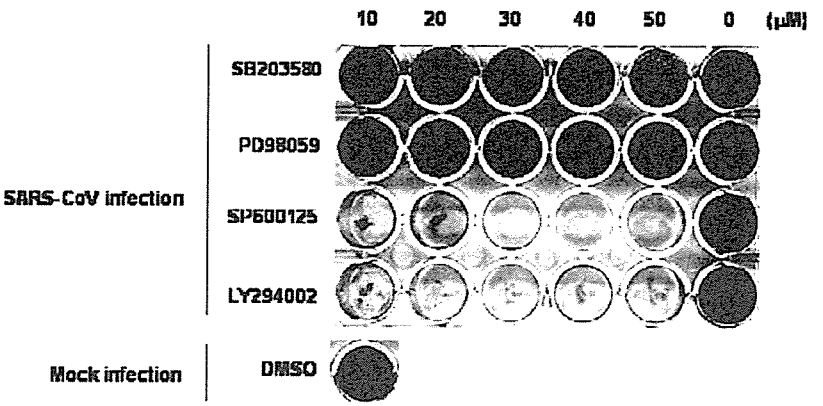

Fig. 6. Effects of signaling pathways on establishing the persistence of Vero E6 cells. SB203580 as a p38 MAPK inhibitor, PD098059 as a MEK inhibitor, and SP600125 as a JNK inhibitor were purchased from Calbiochem (San Diego, CA, USA). LY294002 as a PI3K inhibitor was purchased from Cell Signaling Technology Inc. (Beverly, MA, USA). All reagents were dissolved in dimethyl sulfoxide (DMSO) at a concentration of 10 or 20 mM. All test wells, including mock-treated controls, were treated with DMSO. Vero E6 cells were pre-treated with SB203580, PD98059, SP600125, and LY294002 at concentrations from 10 to 50 μM for 1 h, and then inoculated with SARS-CoV at 2 m.o.i. The plates were fixed and stained at 20 days p.i.

necessary for the establishment of persistence, or for surviving the cells. Both JNK and PI3K/Akt are known to be involved in anti-apoptotic signaling pathways. Especially, our previous study indicated that the activation of Akt signaling pathways is important for anti-apoptosis in SARS-CoV-infected Vero E6 cells [14]. Pro-apoptotic signals, including p38 MAPK, induced cells to undergo apoptosis [13]. In some cell population in Vero E6 cells, anti-apoptotic signals may be stronger than pro-apoptotic signals, resulting in survival.

In the majority of patients infected with hepatitis C virus (HCV), acute infection results in persistent viral replication and the establishment of chronic infection. One viral protein, NS5A, which interacts with receptor binding protein 2 (Grb2), inhibits the activation of ERK1/2 by epidermal growth factor (EGF) [19]. Moreover, NS5A interacts with PI3K (p85), resulting in the promotion of the PI3K/Akt anti-apoptotic signaling pathway [8]. This mechanism may lead to persistent HCV infection in vivo. Tumor necrosis factor-α and interleukin-1β expression, as well as the activities of JNK and activator protein-1 (AP-1), were increased in transgenic mice constitutively expressing HCV core protein [20]. The alternation of cytokine expression and the activation of signaling pathways by core protein may contribute to hepatocarcinogenesis in persistent HCV infection. Thus, viral proteins involve in the activation or inactivation of signaling pathways. Recently, the expression of the nucleocapsid (N) protein of SARS-CoV was shown to induce the up-regulation of AP-1 [7], p38, and JNK, and the down-regulation of ERK and Akt [18]. Although these reports included results obtained in unnatural hosts in vitro, the N protein of SARS-CoV is a candidate for interaction with anti- and pro-apoptotic proteins of host cells. Thus, N protein may also play an important role in the establishment of persistent infection, even though a further experiment is necessary to confirm this hypothesis.

In this paper, we showed a possible mechanism of the establishment of SARS-CoV persistent infection The activation of JNK and PI3K/Akt signaling pathways helps a minor cell population with the potential for persistent infection, to establish persistence. Host gene expression and/or signaling pathways could play important roles in the establishment of persistence. Further investigations are needed to determine the up- or down-regulation of host mRNAs under signaling pathways of JNK and PI3K/Akt in SARS-CoV-infected Vero E6 cells.

Acknowledgements

We thank Drs. Y. Goto (The University of Tokyo, Japan), T. Kenri, Y. Sasaki, F. Taguchi (National Institute of Infectious Diseases, Japan), and O. Inanami (Hokkaido University, Japan) for helpful suggestions. We also thank Ms. M. Ogata (National Institute of Infectious Diseases, Japan) for her assistance. This work was supported, in part, by a grant-in-aid from the Ministry of Health, Labor, and Welfare of Japan and the Japan Health Science Foundation, Tokyo, Japan.

References

[1] B. Adler, H. Adler, H. Pfister, T.W. Jungi, E. Peterhans, Macrophages infected with cytopathic bovine viral diarrhoea virus release a factor(s) capable of priming uninfected macrophages for activation-induced apoptosis, J. Virol. 71 (1997) 3255–3258.

[2] Y. Cai, Y. Liu, D. Yu, X. Zhang, Down-regulation of transcription of the proapoptotic gene BNip3 in cultured astrocytes by murine coronavirus infection, Virology 316 (2003) 104–115.

[3] P. Calain, L. Roux, Generation of measles virus defective interfering particles and their presence in a preparation of attenuated live-virus vaccine, J. Virol. 62 (1988) 2859–2866.

[4] P.K. Chan, K.F. To, A.W. Lo, J.L. Cheung, I. Chu, F.W. Au, J.H. Tong, J.S. Tam, J.J. Sung, H.K. Ng, Persistent infection of SARS coronavirus in colonic cells in vitro, J. Med. Virol. 74 (2004) 1–7.

[5] M.O. Diaz, S. Ziemin, M.M. Le Beau, P. Pitha, S.D. Smith, R.R. Chilcote, J.D. Rowley, Homozygous deletion of the a- and f31-interferon genes in human leukemia and derived cell lines, Proc. Natl. Acad. Sci. U. S. A. 85 (1998) 5259–5263.

[6] H. Diderholm, Z. Dinter, Interference between strains of bovine virus diarrhea virus and their capacity to suppress interferon of a heterologous virus, Proc. Soc. Exp. Biol. 121 (1966) 976–980.

[7] R. He, A. Leeson, A. Andonov, Y. Li, N. Bastien, J. Cao, C. Osiowy, F. Dobie, T. Cutts, M. Ballantine, X. Li, Activation of AP-1 signal transduction pathway by SARS coronavirus nucleocapsid protein, Biochem. Biophys. Res. Commun. 311 (2003) 870–876.

[8] Y. He, H. Nakao, S.L. Tan, S.J. Polyak, P. Neddermann, S. Vijaysri, B.L. Jacobs, M.G. Katze, Subversion of cell signaling pathways by hepatitis C virus nonstructural 5A protein via interaction with Grb2 and P85 phosphatidylinositol 3-kinase, J. Virol. 76 (2002) 9207–9217.

[9] W. Li, M.J. Moore, N. Vasilieva, J. Sui, S.K. Wong, M.A. Berne, M. Somasundaran, J.L. Sullivan, K. Luzuriaga, T.C. Greenough, H. Choe, M. Farzan, Angiotensin-converting enzyme 2 is a functional receptor for the SARS coronavirus, Nature 426 (2003) 450–454.

[10] A. Maeda, M. Hayashi, K. Ishida, T. Mizutani, T. Watanabe, S. Namioka, Characterization of DBT cell clones derived from cells persistently infected with the JHM strain of mouse hepatitis virus, J. Vet. Med. Sci. 57 (1995) 813–817.

[11] M.A. Marra, S.J. Jones, C.R. Astell, R.A. Holt, A. Brooks-Wilson, Y.S. Butterfield, J. Khattra, J.K. Asano, S.A. Barber, S.Y. Chan, A. Cloutier, S.M. Coughlin, D. Freeman, N. Girn, O.L. Griffith, S.R. Leach, M. Mayo, H. McDonald, S.B. Montgomery, P.K. Pandoh, A.S. Petrescu, A.G. Robertson, J.E. Schein, A. Siddiqui, D.E. Smailus, J.M. Stott, G.S. Yang, F. Plummer, A. Andonov, H. Artsob, N. Bastien, K. Bernard, T.F. Booth, D. Bowness, M. Czub, M. Drebot, L. Fernando, R. Flick, M. Garbutt, M. Gray, A. Grolla, S. Jones, H. Feldmann, A. Meyers, A. Kabani, Y. Li, S. Normand, U. Stroher, G.A. Tipples, S. Tyler, R. Vogrig, D. Ward, B. Watson, R.C. Brunham, M. Krajden, M. Petric, D.M. Skowronski, C. Upton, R.L. Roper, The genome sequence of the SARS-associated coronavirus, Science 300 (2003) 1399–1404.

[12] T. Mizutani, H. Inagaki, M. Tada, D. Hayasaka, M. Murphy, T. Fujisawa, J. Hamada, H. Kariwa, I. Takashima, The mechanism of actinomycin D-mediated increase of Borna disease virus (BDV) RNA in cells persistently infected by BDV, Microbiol. Immunol. 44 (2000) 597–603.

[13] T. Mizutani, S. Fukush, M. Saijo, I. Kurane, S. Morikawa, Phosphorylation of p38 MAPK and its downstream targets in SARS coronavirus-infected cells, Biochem. Biophys. Res. Commun. 319 (2004) 1228–1234.

[14] T. Mizutani, S. Fukushi, M. Saijo, I. Kurane, S. Morikawa, Importance of Akt signaling pathway for apoptosis in SARS-CoV-infected Vero E6 cells, Virology 327 (2004) 169–174.
[15] T. Mizutani, S. Fukushi, M. Murakami, T. Hirano, M. Saijo, I. Kurane, S. Morikawa, Tyrosine dephosphorylation of STAT3 in SARS coronavirus-infected Vero E6 cells, FEBS Lett. 577 (2004) 187–192.
[16] S. Perlman, D. Ries, The astrocyte is a target cell in mice persistently infected with mouse hepatitis virus, strain JHM, Microb. Pathog. 3 (1987) 309–314.
[17] P.A. Rota, M.S. Oberste, S.S. Monroe, W.A. Nix, R. Campagnoli, J.P. Icenogle, S. Penaranda, B. Bankamp, K. Maher, M.H. Chen, S. Tong, A. Tamin, L. Lowe, M. Frace, J.L. DeRisi, Q. Chen, D. Wang, D.D. Erdman, T.C. Peret, C. Burns, T.G. Ksiazek, P.E. Rollin, A. Sanchez, S. Liffick, B. Holloway, J. Limor, K. McCaustland, M. Olsen-Rasmussen, R. Fouchier, S. Gunther, A.D. Osterhaus, C. Drosten, M.A. Pallansch, L.J. Anderson, W.J. Bellini, Characterization of a novel coronavirus associated with severe acute respiratory syndrome, Science 300 (2003) 1394–1399.
[18] M. Surjit, B. Liu, S. Jameel, V.T. Chow, S.K. Lal, The SARS coronavirus nucleocapsid (N) protein induces actin reorganization and apoptosis in COS-1 cells in the absence of growth factors, Biochem. J. 383 (2004) 13–18.
[19] S.L. Tan, H. Nakao, Y. He, S. Vijaysri, P. Neddermann, B.L. Jacobs, B.J. Mayer, M.G. Katze, NS5A, a nonstructural protein of hepatitis C virus, binds growth factor receptor-bound protein 2 adaptor protein in a Src homology 3 domain/ligand-dependent manner and perturbs mitogenic signaling, Proc. Natl. Acad. Sci. U. S. A. 96 (1999) 5533–5538.
[20] T. Tsutsumi, T. Suzuki, K. Moriya, H. Yotsuyanagi, Y. Shintani, H. Fujie, Y. Matsuura, S. Kimura, K. Koike, T. Miyamura, Alteration of intrahepatic cytokine expression and AP-1 activation in transgenic mice expressing hepatitis C virus core protein, Virology 304 (2002) 415–424.

Available online at www.sciencedirect.com
SCIENCE DIRECT®
Antiviral Research 66 (2005) 159–163
Antiviral Research
www.elsevier.com/locate/antiviral

Short communication

Inhibitory effect of mizoribine and ribavirin on the replication of severe acute respiratory syndrome (SARS)-associated coronavirus

Masayuki Saijo[a,*], Shigeru Morikawa[a], Shuetsu Fukushi[a], Tetsuya Mizutani[a], Hideki Hasegawa[b], Noriyo Nagata[b], Naoko Iwata[b], Ichiro Kurane[a]

[a] *Special Pathogens Laboratory, Department of Virology 1, National Institute of Infectious Diseases, Tokyo 208-0011, Japan*
[b] *Laboratory of Infectious Disease Pathology, Department of Pathology, National Institute of Infectious Diseases, Tokyo 208-0011, Japan*

Received 21 May 2004; accepted 14 January 2005

Abstract

The activity of inosine-5′-monophosphate dehydrogenase (IMPDH) inhibitors, mizoribine and ribavirin, against severe acute respiratory syndrome (SARS)-associated coronavirus (SARS-CoV) was determined by plaque reduction and yield reduction assays. Mizoribine and ribavirin selectively inhibited replication of SARS-CoV. The 50% inhibitory concentration (IC_{50}) of mizoribine for SARS-CoV Frankfurt-1 and SARS-CoV HKU39849, as determined by plaque reduction was 3.5 μg/ml and 16 μg/ml, respectively, and the IC_{50} of ribavirin for SARS-CoV Frankfurt-1 and SARS-CoV HKU39849 was 20 μg/ml and 80 μg/ml, while the 50% cytotoxic concentration of mizoribine and ribavirin for Vero E6 cells exceeded 200 μg/ml. In a yield reduction assay, mizoribine (10 μg/ml) and ribavirin (40 μg/ml) inhibited the replication of SARS-CoV and reduced the infectious SARS-CoV titers to one-tenth or less. Mizoribine inhibited replication of SARS-CoV more strongly than ribavirin. However, neither drug could completely inhibit replication of SARS-CoV even at concentrations up to 100 μg/ml.

Keywords: SARS; Coronavirus; Ribavirin; Mizoribine

The first outbreak of severe acute respiratory syndrome (SARS) occurred in the Guangdong Province, in Southern China, in November 2002, and then spread through human-to-human infection from there to other areas of China, as well as Vietnam, Singapore, Canada and some 30 countries (Lee et al., 2003; Poutanen et al., 2003; Tsang et al., 2003). Approximately 8000 SARS patients have been reported and about 800 patients died in the outbreak from November 2002 and July 2003. SARS-associated coronavirus (SARS-CoV) has been identified as the causative agent for SARS (Drosten et al., 2003; Ksiazek et al., 2003).

In the present study, inhibitory effect of mizoribine (4-carbamoyl-1-β-D-ribofuranosylimidazolium-5-olate, M_w 259.22) and ribavirin (1-β-D-ribofuranosyl-1,2,4-triazole-3-carboxamide, M_w 244.2) on the replication of SARS-CoV was evaluated. Mizoribine, an imidazole nucleoside, is an immunosuppressive agent used for renal transplantation, autoimmune diseases and steroid-resistant nephrotic syndrome in Japan. Mizoribine is phosphorylated by adenosine kinase and converted its active form, mizoribine 5′-monophosphate. This activated form of mizoribine acts as an inhibitor of the enzyme, inosine 5′-monophosphate dehydrogenase (IMPDH) and guanosine monophosphate synthetase, both enzymes being essential to the synthesis of guanosine monophosphate from inosine monophosphate through the de novo pathway (Yokota, 2002). Furthermore, mizoribine possesses in vitro anti-viral activities against herpes simplex virus, cytomegalovirus, respiratory syncytial virus, influenza viruses, and bovine viral diarrhea virus (Shiraki et al., 1990; Hosoya et al., 1993; Shigeta, 2000; Pancheva et al., 2002; Stuyver et al., 2002). Ribavirin is a well-known broad-spectrum antiviral agent. Ribavirin 5′-monophosphate, a metabolite of ribavirin, also acts as an inhibitor of IMPDH.

Mizoribine and ribavirin were supplied from Yamasashouyu Co., Ltd., Choshi, Chiba, Japan. The cytotoxic effect, cytotoxic concentration (CC) of mizoribine and ribavirin for Vero E6 cells (American Type Cell Collection, Manas-

* Corresponding author. Tel.: +81 42 561 0771; fax: +81 42 561 2039.
E-mail address: msaijo@nih.go.jp (M. Saijo).

0166-3542/$ – see front matter © 2005 Elsevier B.V. All rights reserved.
doi:10.1016/j.antiviral.2005.01.003

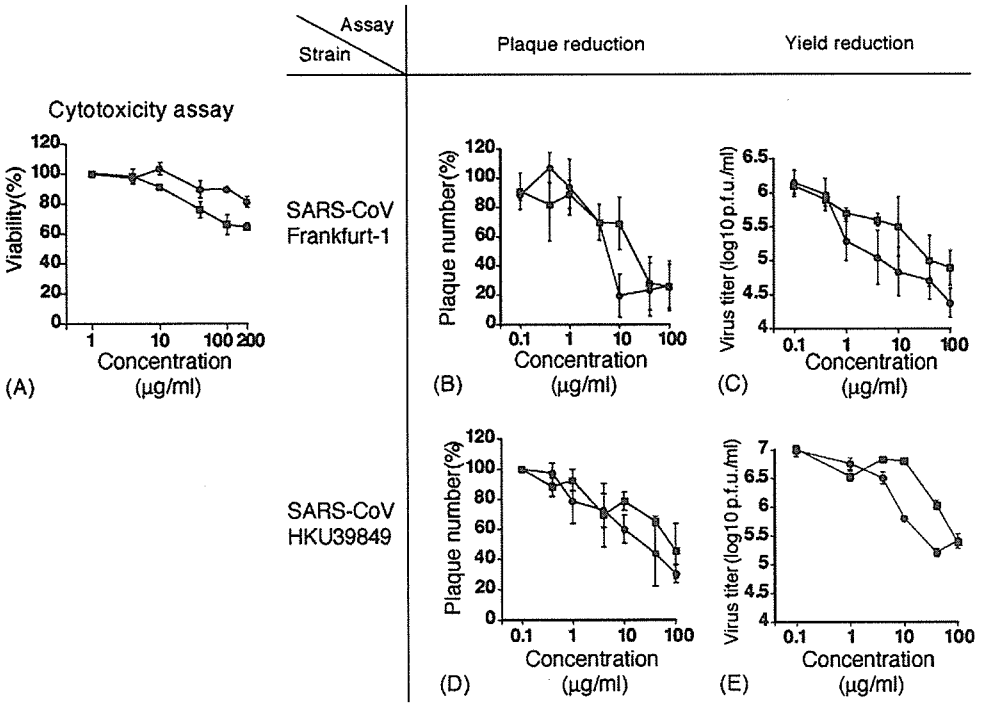

Fig. 1. Cytotoxicity (A), inhibitory effect on plaque formation of SARS-CoV Frankfurt-1 (B) and HKU39849 (D) in a plaque reduction assay and inhibitory effect on replication of SARS-CoV Frankfurt-1 (C) and HKU39849 (E) in yield reduction assay. The symbols, "●" and "■" represent mizoribine and ribavirin, respectively. The vertical bar indicates 1 S.D. One hundred percent of plaque numbers in (B) and (D) correspond to the control (no compound). The SARS-CoV titers at 0 μg/ml of drugs are not shown in these figures, as these titers were not significantly different from those at a concentration of 0.1 μg/ml.

sas, VA.) was measured using a WST-1 cytotoxicity assay kit (Roche Diagnositics, Mannheim, Germany), according to the manufacturer's instructions. The CC_{50} and CC_{20} were defined as the concentration at which the viability of Vero E6 cells decreased to 50% and 80% of that of cells cultured without the addition of antiviral drugs, respectively. In the cytotoxicity assay, Vero E6 cells were cultured in Eagle's minimum essential medium (MEM) containing 2% fetal bovine serum (FBS), penicillin G, and streptomycin (MEM-2FBS), which was the same medium for growth of SARS-CoV. Briefly, approximately 10^4 of Vero E6 cells per well were inoculated in each well in a 96-well microplate and let stand for 4 h to allow the cells to adhere to the bottom of the wells. The culture medium was then replaced by the MEM-2FBS with or without drug. The cells were cultured for 3 days in a CO_2 incubator under humidified condition, and then evaluated for cytotoxicity using the WST-1 kit. The level of Vero E6 cells' viability at different concentration of either drug is shown in Fig. 1A. The CC_{50} of mizoribine and ribavirin exceed at 200 μg/ml, and the CC_{20} of mizoribine and ribavirin was 200 and 40 μg/ml, respectively.

In the present study, two strains of SARS-CoV (Frankfurt-1 and HKU39849) were used. SARS-CoV (Frankfurt-1) and SARS-CoV (HKU39849) were kindly provided by Dr. John Ziebuhr of the Institute of Virology and Immunology, University of Wuerzburg, Wuerzburg, Germany, and Dr. J.S. Malik Peiris, Department of Microbiology, Hong Kong University, HKSAR, respectively. The anti-SARS-CoV activity of these drugs was firstly measured by a plaque reduction assay in Vero E6 cells. Vero E6 cell monolayers seeded in 24-well microplates were inoculated with 0.2 ml of SARS-CoV stock solution at 100 plaque formation unit (p.f.u.)/ml. After a 1-h incubation, the inocula were removed and the cells were washed with phosphate-buffered saline solution (PBS). The cells were then cultured in MEM-2FBS with a designated concentration of each compound and 0.5% methylcellulose for 48 h in a CO_2 incubator under humidified conditions. The culture medium was then removed and the cells in the culture plate were fixed with a 10% formalin solution and stained with crystal violet solution. The plaque number was then counted. The incubation time was set at 48 h, because the plaque size became too large to be counted when the incubation time was set at 3 days or more. The experiment was performed in duplicate. The 50% inhibitory concentration (IC_{50}) was defined as the concentration at which the plaque number decreased to half of that in cells cultured without addition of antiviral drugs. The same experiment was performed three times independently for each drug and the IC_{50} values were calculated as the average ± standard deviation (SD) of the three experiments. The 20% inhibitory concentration (IC_{20}) and 80% inhibitory concentration (IC_{80}) were determined as well. The inhibitory effect of mizoribine and ribavirin on SARS-CoV (Frankfurt-1 and HKU39849)-plaque formation is shown in Fig. 1B and D, respectively. The IC_{50}, IC_{20} and IC_{80} values of mizoribine and ribavirin for SARS-CoV are shown in Table 1, and so are the cytotoxic concentrations. Re-

Table 1
Inhibitory concentrations of mizoribine and ribavirin on SARS-CoV Frankfurt-1 and HKU39849 strains

Drug	SARS-CoV strain	Inhibitory concentration (μg/ml)			Cytotoxic concentration (μg/ml)	
		IC_{20}	IC_{50}	IC_{80}	CC_{20}	CC_{50}
Mizoribine	Frankfurt-1	2.2 ± 2.0	3.5 ± 2.9	>100	200	>200
	HKU39849	1.4 ± 0.6	16 ± 2.8	>100		
Ribavirin	Frankfurt-1	8.9 ± 6.3	20 ± 15	>100	40	>200
	HKU39849	15 ± 1.4	80 ± 28	>100		

duction in the number of plaques was demonstrated in cells cultured in medium to which mizoribine or ribavirn were added. However, IC_{80} values of both drugs could not be determined, because plaque formation by SARS-CoV Frankfurt-1 and HKU39849 was not completely inhibited even at a concentration of 100 μg/ml of each drug (Fig. 1B and D). As shown in Fig. 1B and D, mizoribine inhibited plaque formation by SARS-CoV more strongly than ribavirin in plaque reduction assay. The size of plaques was significantly decreased at a concentration of 10 μg/ml or greater for each drug (data not shown).

The inhibitory effects of mizoribine and ribavirin on SARS-CoV replication were further evaluated by a yield reduction assay. Vero E6 cells seeded in 6-well microplates were inoculated with SARS-CoV solution for 1 h to allow infection with SARS-CoV at a multiplicity of infection (m.o.i.) of 0.01 p.f.u./cell. After 1 h, the inocula were removed and the cells were washed twice with PBS and cultured in MEM-2FBS with or without drug for 20 h. The time between inoculation of SARS-CoV and harvesting samples was 20 h, because the preliminary study revealed that the growth of SARS-CoV was so fast that 2 or more days-incubation made it difficult to assess an inhibitory effect of mizoribine and ribavirin on SARS-CoV replication. Therefore, a 20-h incubation time was set in the yield reduction assays. The medium was then collected and stored in −80 °C until use. At this stage, no obvious specific cytopathic effect was observed (data not shown). In each experiment, two wells were used at each concentration of the antiviral drugs. The infectious dose of SARS-CoV was determined by a plaque assay in Vero E6 cells. The same experiment was conducted three times independently and the infectious dose was calculated as the average ± S.D. of the three independent experiments. Mizoribine inhibited replication of SARS-CoV (Frankfurt-1 and HKU39849), and the infectious viral dose at the concentration of 10 μg/ml decreased to one-tenth or less of the control (Fig. 1C and E). The inhibitory effect of mizoribine on SARS-CoV replication was greater than that of ribavirin (Fig. 1C and E).

In both plaque reduction and yield reduction assays, it was demonstrated that mizoribine inhibited replication of SARS-CoV more strongly than ribavirin. In order to determine whether the difference in the degree of inhibitory effect between mizoribine and ribavirin on SARS-CoV was a phenomenon observed only for SARS-CoV, the inhibitory effect of these drugs on replication of vaccinia virus (Lister strain) and herpes simplex virus type 1 (VR-3 strain), which were stored in the National Institute of Infectious Diseases, Tokyo, Japan, was measured as a control by plaque reduction assay in Vero E6 cells. It has been reported that ribavirin inhibits replication of vaccinia virus (Kirsi et al., 1983). The plaque reduction assay for vaccinia virus and HSV-1 was carried out as described above for SARS-CoV except for the length of the culture period. In the plaque reduction assay for vaccinia virus and HSV-1, the cells were cultured for 4 days. As shown in Fig. 2A, ribavirin inhibited replication of vaccinia virus to the same extent as mizoribine. However, ribavirin did not show anti-HSV-1 activity in Vero E6 cells, while mizoribine showed an inhibitory effect on the replication of HSV-1 (Fig. 2B). These results suggested that the difference in degree of inhibitory effect on viral replication between mizoribine and ribavirin was dependent on the type of virus and that the mode of antiviral action of mizoribine was not the same as that of ribavirin, although both drugs act as IMPDH inhibitors.

During the outbreak of SARS in 2003, several therapeutic strategies for the treatment of SARS were tried, such as administration of ribavirin, lopinavir/ritonavir (a protease inhibitor), interferon, steroids, and so on, alone or in combination with each other (Ho et al., 2003; Loutfy et al., 2003; Zhao et al., 2003; Zhaori, 2003; Chu et al., 2004). However, no efficacious treatments of SARS with antiviral agents have been developed. Several compounds, such as ribavirin, lopinavir/ritonavir, 6-azauridine, pyrazofurin, interferon-α, interferon-β, glycyrrhizin, niclosamide (antihelminthic drug), aurintricarboxylic acid, nelfinavir (HIV protease inhibitor), *S*-nitroso-*N*-acetylpenicillamine (a nitric oxide donor), and chloroquine (antimalaria drug) were demonstrated to show anti-SARS-CoV activity in vitro (Cinatl et al., 2003; Chu et al., 2004; He et al., 2004; Hensley et al., 2004; Keyaerts et al., 2004; Sainz et al., 2004; Stroher et al., 2004; Wu et al., 2004; Yamamoto et al., 2004).

Cinatl et al. (2003) reported that ribavirin did not have anti-SARS-CoV activity in vitro. Also in the present study ribavirin did not completely inhibit replication of SARS-CoV even at a concentration of 100 μg/ml. However, ribavirin did possess an inhibitory effect on replication of SARS-CoV, as demonstrated in our present study as well as that of Chu et al. (2004). Scoring of cytopathogenicity was performed in the former study to determine the antiviral activity of the tested compounds (Cinatl et al., 2003), while plaque reduction assay was performed in the present studies and those of Chu et al.

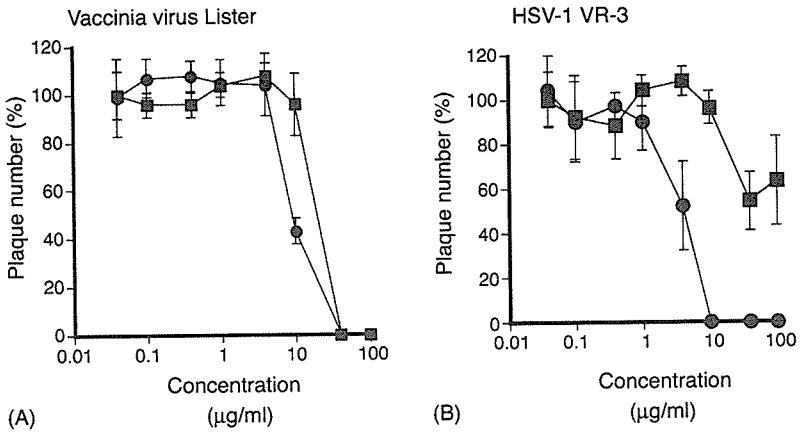

Fig. 2. Inhibitory effect of mizoribine (●) and ribavirin (■) on vaccinia virus (Lister strain) (A) and HSV-1 VR-3 (B) determined by plaque reduction assay. The vertical bar indicates 1 S.D. calculated from the data obtained by independent three experiments. One hundred percent of plaque numbers correspond to the control (no compound).

(2004). The reason why an inhibitory effect of ribavirin was demonstrated in the present study and not in the previous study by Cinatl et al. (2003) may be attributed to difference in the procedures used, and, in particular, to the duration of the incubation times of the cells in the presence of ribavirin.

Ribavirin is phosphorylated to form ribavirin mono-, di- and triphosphate. Ribavirin-monophosphate inhibits the enzymatic activity of IMPDH, resulting in decreased intracellular guanosine triphosphate and deoxyguanosine triphosphate pool levels (Streeter et al., 1973). This alteration in guanosine triphosphate pool levels causes suppression in cellular DNA, mRNA and protein synthesis. Possible mechanisms of antiviral activity of ribavirin were reported for rotavirus, vesicular stomatitis virus, influenza virus and vaccinia virus (Eriksson et al., 1977; Lowe et al., 1977; Muller et al., 1977; Goswami et al., 1979; Smee et al., 1982; Kirsi et al., 1983; Toltzis et al., 1988). As described above, the mode of antiviral action of mizoribine is considered to be similar, but not identical to that of ribavirin, although both drugs act as IMPDH inhibitors. The mechanism of anti-SARS-CoV activity of mizoribine and ribavirin should be addressed in future studies.

In summary, mizoribine and ribavirin possess an inhibitory effect on the replication of SARS-CoV in vitro, but their anti-SARS-CoV activity is virustatic rather than virucidal. The findings obtained in the present study do not legitimate the use of ribavirin or mizoribine for the treatment of patients with SARS, but may contribute to the further development of antiviral agents for SARS-CoV and of therapeutic strategies for SARS.

Acknowledgements

We thank Dr. J. Ziebuhr of the Institute of Virology and Immunology, University of Wuerzburg, Wuerzburg, Germany, and Dr. J.S. Malik Peiris, Department of Microbiology, Hong Kong University, HKSAR, for kindly providing with SARS-CoV Frankfult-1 strain and HKU39849 strain, respectively. We also thank Dr. H. Machida and Dr. N. Ashida, of the Yamasa-shouyu Co., Ltd., Choshi, Chiba, Japan, for kindly providing mizoribine and ribavirin. We also thank Ms. M. Ogata for her technical and official assistance. The study was partly supported by a Grants-in-Aids from the Ministry of Health, Labor and Welfare of Japan.

References

Chu, C.M., Cheng, V.C., Hung, I.F., Wong, M.M., Chan, K.H., Chan, K.S., Kao, R.Y., Poon, L.L., Wong, C.L., Guan, Y., Peiris, J.S., Yuen, K.Y., 2004. Role of lopinavir/ritonavir in the treatment of SARS: initial virological and clinical findings. Thorax 59, 252–256.

Cinatl, J., Morgenstern, B., Bauer, G., Chandra, P., Rabenau, H., Doerr, H.W., 2003. Glycyrrhizin, an active component of liquorice roots, and replication of SARS-associated coronavirus. Lancet 361, 2045–2046.

Drosten, C., Gunther, S., Preiser, W., van der Werf, S., Brodt, H.R., Becker, S., Rabenau, H., Panning, M., Kolesnikova, L., Fouchier, R.A., Berger, A., Burguiere, A.M., Cinatl, J., Eickmann, M., Escriou, N., Grywna, K., Kramme, S., Manuguerra, J.C., Muller, S., Rickerts, V., Sturmer, M., Vieth, S., Klenk, H.D., Osterhaus, A.D., Schmitz, H., Doerr, H.W., 2003. Identification of a novel coronavirus in patients with severe acute respiratory syndrome. N. Engl. J. Med. 348, 1967–1976.

Eriksson, B., Helgstrand, E., Johansson, N.G., Larsson, A., Misiorny, A., Noren, J.O., Philipson, L., Stenberg, K., Stening, G., Stridh, S., Öberg, B., 1977. Inhibition of influenza virus ribonucleic acid polymerase by ribavirin triphosphate. Antimicrob. Agents Chemother. 11, 946–951.

Goswami, B.B., Borek, E., Sharma, O.K., Fujitaki, J., Smith, R.A., 1979. The broad spectrum antiviral agent ribavirin inhibits capping of mRNA. Biochem. Biophys. Res. Commun. 89, 830–836.

He, R., Adonov, A., Traykova-Adonova, M., Cao, J., Cutts, T., Grudesky, E., Deschambaul, Y., Berry, J., Drebot, M., Li, X., 2004. Potent and selective inhibition of SARS coronavirus replication by aurintricarboxylic acid. Biochem. Biophys. Res. Commun. 320, 1199–1203.

Hensley, L.E., Fritz, L.E., Jahrling, P.B., Karp, C.L., Huggins, J.W., Geisbert, T.W., 2004. Interferon-beta 1a and SARS coronavirus replication. Emerg. Infect. Dis. 10, 317–319.

Ho, J.C., Ooi, G.C., Mok, T.Y., Chan, J.W., Hung, I., Lam, B., Wong, P.C., Li, P.C., Ho, P.L., Lam, W.K., Ng, C.K., Ip, M.S., Lai, K.N., Chan-Yeung, M., Tsang, K.W., 2003. High-dose pulse versus nonpulse corticosteroid regimens in severe acute respiratory syndrome. Am. J. Respir. Crit. Care Med. 168, 1449–1456.

Hosoya, M., Shigeta, S., Ishii, T., Suzuki, H., De Clercq, E., 1993. Comparative inhibitory effects of various nucleoside and nonnucleoside analogues on replication of influenza virus types A and B in vitro and in ovo. J. Infect. Dis. 168, 641–646.

Keyaerts, E., Vijgen, L., Chen, L., Maes, P., Hedenstierna, G., Van Ranst, M., 2004. Inhibition of SARS-coronavirus infection in vitro by *S*-nitroso-*N*-acetylpenicillamine, a nitric oxide donor compound. Int. J. Infect. Dis. 8, 223–226.

Kirsi, J.J., North, J.A., McKernan, P.A., Murray, B.K., Canonico, P.G., Huggins, J.W., Srivastava, P.C., Robins, R.K., 1983. Broad-spectrum antiviral activity of 2-beta-D-ribofuranosylselenazole-4-carboxamide, a new antiviral agent. Antimicrob. Agents Chemother. 24, 353–361.

Ksiazek, T.G., Erdman, D., Goldsmith, C.S., Zaki, S.R., Peret, T., Emery, S., Tong, S., Urbani, C., Comer, J.A., Lim, W., Rollin, P.E., Dowell, S.F., Ling, A.E., Humphrey, C.D., Shieh, W.J., Guarner, J., Paddock, C.D., Rota, P., Fields, B., DeRisi, J., Yang, J.Y., Cox, N., Hughes, J.M., LeDuc, J.W., Bellini, W.J., Anderson, L.J., 2003. A novel coronavirus associated with severe acute respiratory syndrome. N. Engl. J. Med. 348, 1953–1966.

Lee, N., Hui, D., Wu, A., Chan, P., Cameron, P., Joynt, G.M., Ahuja, A., Yung, M.Y., Leung, C.B., To, K.F., Lui, S.F., Szeto, C.C., Chung, S., Sung, J.J., 2003. A major outbreak of severe acute respiratory syndrome in Hong Kong. N. Engl. J. Med. 348, 1986–1994.

Loutfy, M.R., Blatt, L.M., Siminovitch, K.A., Ward, S., Wolff, B., Lho, H., Pham, D.H., Deif, H., LaMere, E.A., Chang, M., Kain, K.C., Farcas, G.A., Ferguson, P., Latchford, M., Levy, G., Dennis, J.W., Lai, E.K., Fish, E.N., 2003. Interferon alfacon-1 plus corticosteroids in severe acute respiratory syndrome: a preliminary study. JAMA 290, 3222–3228.

Lowe, J.K., Brox, L., Henderson, J.F., 1977. Consequences of inhibition of guanine nucleotide synthesis by mycophenolic acid and virazole. Cancer Res. 37, 736–743.

Muller, W.E., Maidhof, A., Taschner, H., Zahn, R.K., 1977. Virazole (1-beta-D-ribofuranosyl-1,2,4-triazole-3-carboxamide); a cytostatic agent. Biochem. Pharmacol. 26, 1071–1075.

Pancheva, S., Dundarova, D., Remichkova, M., 2002. Potentiating effect of mizoribine on the anti-herpes virus activity of acyclovir. Z. Naturforsch. [C] 57, 902–904.

Poutanen, S.M., Low, D.E., Henry, B., Finkelstein, S., Rose, D., Green, K., Tellier, R., Draker, R., Adachi, D., Ayers, M., Chan, A.K., Skowronski, D.M., Salit, I., Simor, A.E., Slutsky, A.S., Doyle, P.W., Krajden, M., Petric, M., Brunham, R.C., McGeer, A.J., 2003. Identification of severe acute respiratory syndrome in Canada. N. Engl. J. Med. 348, 1995–2005.

Sainz Jr., B., Mossel, E.C., Peters, C.J., Garry, R.F., 2004. Interferon-beta and interferon-gamma synergistically inhibit the replication of severe acute respiratory syndrome-associated coronavirus (SARS-CoV). Virology 329, 11–17.

Shigeta, S., 2000. Recent progress in antiviral chemotherapy for respiratory syncytial virus infections. Expert Opin. Investig. Drugs 9, 221–235.

Shiraki, K., Ishibashi, M., Okuno, T., Kokado, Y., Takahara, S., Yamanishi, K., Sonoda, T., Takahashi, M., 1990. Effects of cyclosporine, azathioprine, mizoribine, and prednisolone on replication of human cytomegalovirus. Transplant. Proc. 22, 1682–1685.

Smee, D.F., Sidwell, R.W., Clark, S.M., Barnett, B.B., Spendlove, R.S., 1982. Inhibition of rotaviruses by selected antiviral substances: mechanisms of viral inhibition and in vivo activity. Antimicrob. Agents Chemother. 21, 66–73.

Streeter, D.G., Witkowski, J.T., Khare, G.P., Sidwell, R.W., Bauer, R.J., Robins, R.K., Simon, L.N., 1973. Mechanism of action of 1-β-D-ribofuranosyl-1,2,4-triazole-3-carboxamide (Virazole), a new broad-spectrum antiviral agent. Proc. Natl. Acad. Sci. U.S.A. 70, 1174–1178.

Stroher, U., DiCaro, A., Li, Y., Strong, J.E., Aoki, F., Plummer, F., Jones, S.M., Feldmann, H., 2004. Severe acute respiratory syndrome-related coronavirus is inhibited by interferon-alpha. J. Infect. Dis. 189, 1164–1167.

Stuyver, L.J., Lostia, S., Patterson, S.E., Clark, J.L., Watanabe, K.A., Otto, M.J., Pankiewicz, K.W., 2002. Inhibitors of the IMPDH enzyme as potential anti-bovine viral diarrhoea virus agents. Antiviral Chem. Chemother. 13, 345–352.

Toltzis, P., O'Connell, K., Patterson, J.L., 1988. Effect of phosphorylated ribavirin on vesicular stomatitis virus transcription. Antimicrob. Agents Chemother. 32, 492–497.

Tsang, K.W., Ho, P.L., Ooi, G.C., Yee, W.K., Wang, T., Chan-Yeung, M., Lam, W.K., Seto, W.H., Yam, L.Y., Cheung, T.M., Wong, P.C., Lam, B., Ip, M.S., Chan, J., Yuen, K.Y., Lai, K.N., 2003. A cluster of cases of severe acute respiratory syndrome in Hong Kong. N. Engl. J. Med. 348, 1977–1985.

Wu, C.J., Jan, J.T., Chen, C.M., Hsieh, H.P., Hwang, D.R., Liu, H.W., Liu, C.Y., Huang, H.W., Chen, S.C., Hong, C.F., Lin, R.K., Chao, Y.S., Hsu, J.T., 2004. Inhibition of severe acute respiratory syndrome coronavirus replication by niclosamide. Antimicrob. Agents Chemother. 48, 2693–2696.

Yamamoto, N., Yang, R., Yoshinaka, Y., Amari, S., Nakano, T., Cinatl, J., Rabenau, H., Doerr, H.W., Hunsmann, G., Otaka, A., Tamamura, H., Fujii, N., Yamamoto, N., 2004. HIV protease inhibitor nelfinavir inhibits replication of SARS-associated coronavirus. Biochem. Biophys. Res. Commun. 318, 719–725.

Yokota, S., 2002. Mizoribine: mode of action and effects in clinical use. Pediatr. Int. 44, 196–198.

Zhao, Z., Zhang, F., Xu, M., Huang, K., Zhong, W., Cai, W., Yin, Z., Huang, S., Deng, Z., Wei, M., Xiong, J., Hawkey, P.M., 2003. Description and clinical treatment of an early outbreak of severe acute respiratory syndrome (SARS) in Guangzhou, PR China. J. Med. Microbiol. 52, 715–720.

Zhaori, G., 2003. Antiviral treatment of SARS: can we draw any conclusions. CMAJ 169, 1165–1166.

Jpn. J. Infect. Dis., 58, 88-94, 2005

Original Article

Immunological Detection of Severe Acute Respiratory Syndrome Coronavirus by Monoclonal Antibodies

Kazuo Ohnishi, Masahiro Sakaguchi, Tomohiro Kaji, Kiyoko Akagawa, Tadayoshi Taniyama, Masataka Kasai, Yasuko Tsunetsugu-Yokota, Masamichi Oshima, Kiichi Yamamoto, Naomi Takasuka, Shu-ichi Hashimoto, Manabu Ato, Hideki Fujii, Yoshimasa Takahashi, Shigeru Morikawa[1], Koji Ishii[2], Tetsutaro Sata[4], Hirotaka Takagi[5], Shigeyuki Itamura[3], Takato Odagiri[3], Tatsuo Miyamura[2], Ichiro Kurane[1], Masato Tashiro[3], Takeshi Kurata[6], Hiroshi Yoshikura[6] and Toshitada Takemori*

Department of Immunology, [1]Department of Virology I, [2]Department of Virology II, [3]Department of Virology III, [4]Department of Pathology and [5]Division of Biosafety Control and Research, [6]National Institute of Infectious Diseases, Tokyo 162-8640, Japan

(Received October 20, 2004. Accepted February 14, 2005)

SUMMARY: In order to establish immunological detection methods for severe acute respiratory syndrome coronavirus (SARS-CoV), we established monoclonal antibodies directed against structural components of the virus. B cell hybridomas were generated from mice that were hyper-immunized with inactivated SARS-CoV virion. By screening 2,880 generated hybridomas, we established three hybridoma clones that secreted antibodies specific for nucleocapsid protein (N) and 27 clones that secreted antibodies specific for spike protein (S). Among these, four S-protein specific antibodies had in vitro neutralization activity against SARS-CoV infection. These monoclonal antibodies enabled the immunological detection of SARS-CoV by immunofluorescence staining, Western blot or immunohistology. Furthermore, a combination of monoclonal antibodies with different specificities allowed the establishment of a highly sensitive antigen-capture sandwich ELISA system. These monoclonal antibodies would be a useful tool for rapid and specific diagnosis of SARS and also for possible antibody-based treatment of the disease.

INTRODUCTION

The outbreak of severe acute respiratory syndrome (SARS) in 2003, caused by SARS coronavirus (SARS-CoV)(1,2), ultimately led to 8,000 people becoming infected, 916 of whom died (3; http://who.int/csr/sars/country/en/country2003_08_15.pdf). Even though the WHO announced an end to the epidemic (4; http://www.who.int/entity/csr/sars/resources/en/SARSReferenceLab1.pdf), the threat of re-emergence persists due to the absence of a vaccine, and inability of health services to rapidly detect and specifically diagnose the disease. One of the critical issues in the management of clinical patients and control of the pandemic is a system of early diagnosis that distinguishes SARS from other types of pulmonary infections. As an epidemiological history of contact with SARS patients is not always provable and there are no clinical signs unique to SARS patients (5), confirmatory diagnosis relies primarily on laboratory tests.

To date, viral shedding of SARS-CoV has been extensively studied to improve diagnosis and infectious control (6-8). Maximum virus shedding takes place between day 12 and day 14 of disease onset. For most acute respiratory viral infections, viral shedding occurs within the first few days from the nasopharyngeal tissue and soon after at the upper respiratory tract, but seldom lasts for more than 10 days (6-8). The peak of shedding in stools occurs a few days after respiratory shedding and remains high even after 3 weeks (7, 8). SARS-CoV was detected in patients' plasma samples within several days of the onset of fever, sometimes at levels equivalent to those recorded for nasopharyngeal aspirates (6, 9).

Previously, during the outbreak in Hong Kong (8), laboratory diagnosis for SARS virus infection was based on a combination of serologic tests, reverse transcription-polymerase chain reaction (RT-PCR), and virus isolation. IgG seroconversion among those infected was 93% by day 28 (5), suggesting that while antibody seroconversion provides reliable proof of infection (5,10); it is, however, not suitable for early diagnosis (11). Among patients in whom the serological evidence could be retrospectively examined, RT-PCR provided about 60% of the diagnostic yield using tracheal aspirates and stools for the first 2 weeks after the onset of illness (8). Although the availability of data that compares the diagnostic yield of various specimen types is still limited, it has been suggested that a combination of stool samples and pooled throat and nasal swab specimens provides reagents for safe and high-yield SARS-CoV detection (8). Furthermore, in addition to RT-PCR on respiratory and fecal samples, serology is needed to confirm the diagnosis of SARS-CoV infection in most cases.

Based on clinical experience, several options have been considered in the quest to develop the capacity to accurately diagnose SARS-CoV infection, including molecular biology techniques and serological tests such as antigen-captured ELISA assay and immunofluorescence assay to detect virus-infected cells in respiratory swabs (5-12). The preparation of monoclonal antibodies (mAbs) is considered to be valuable especially for serological testing.

*Corresponding author: Mailing address: Department of Immunology, National Institute of Infectious Diseases, Toyama 1-23-1, Shinjuku-ku, Tokyo 162-8640, Japan. Tel: +81-3-5285-1111, Fax: +81-5285-1150, E-mail: ttoshi@nih.go.jp

In this paper we report the successful establishment and the characterization of mAbs against SARS-CoV structural components. These mAbs enabled the general immunological detection of SARS-CoV, by the methods such as immunofluorescent staining, Western blotting, and immunohistology, in addition to the construction of highly sensitive antigen-capture sandwich ELISA.

MATERIALS AND METHODS

Virus and cell culture: SARS-CoV (HKU-39849) was kindly supplied by Dr. J. S. M. Peiris, Department of Microbiology, the University of Hong Kong. The live virus was manipulated under the physical containment level P3. For the purification of the virion, the day-2 culture supernatant of Vero E6, which had been infected with SARS-CoV at moi = 1.0, was centrifuged at 8,000×g for 30 min to remove cell debris. The virion in the supernatant was precipitated with 8% polyethylene glycol/ 0.5 M NaCl, and further purified by 20%/60%-discontinuous sucrose density gradient centrifugation. This fraction was inactivated by UV-irradiation (260 nm, 4.75 J/cm^2), and used as UV-inactivated SARS-CoV fraction. We and others confirmed that this condition completely inactivates SARS-CoV (13,14).

Production of mAbs: BALB/c mice (9-week old females, Japan SLC) were immunized subcutaneously with 20 μg of UV-inactivated SARS-CoV using Freund's Complete Adjuvant (FCA, Sigma, St. Louis, Mo., USA). After 2 weeks, the mice were boosted with a subcutaneous injection of 5 μg of UV-inactivated SARS-CoV using Freund's Incomplete Adjuvant (FIA, Sigma). On day-3 after the boost, sera from the mice were tested by ELISA for the antibody titer against SARS-CoV. The two mice showing highest antibody titer were further boosted intravenously with 5 μg of the inactivated virus 14 days after the previous boost. This immunization schedule was called protocol-1. In protocol-2 the booster injection was repeated two more times before the final boost. Three days after the final boost, spleens from two mice were excised and the splenocytes were fused with Sp2/O-Ag14 myeloma by the polyethylene glycol method of Kozbor and Roder (15). The fused cells from the two spleens were cultured and HAT-selected on twenty 96-well plates. The first screening was conducted by ELISA using SARS-CoV infected Vero E6 cell lysate as the antigen. In this first screening, the ELISA with uninfected Vero E6 cell lysate was used as the negative control. After the virus was inactivated by UV-irradiation, cell lysates were prepared by NP-40 lysis buffer (1% NP-40/ 150 mM NaCl/ 50 mM Tris, pH 7.5) followed by centrifugation at 15,000 rpm for 20 min to remove the cell debris. The supernatant was diluted 100-fold using ELISA-coating buffer (50 mM sodium bicarbonate, pH 9.6) and the ELISA plates (Dynatech, Chantily, Va., USA) were coated at 4°C overnight. After blocking with 1% ovalbumin in PBS-Tween (10 mM phosphate buffer, 140 mM NaCl, 0.05% Tween 20, pH 7.5) for 1 h, the culture supernatants from HAT-selected hybridomas were added and incubated for 1 h. After washing with PBS-Tween, the bound antibodies were detected with alkaline phosphatase-conjugated anti-mouse IgG (1:2000, Zymed, South San Francisco, Calif., USA) using *p*-nitrophenyl phosphate (PNPP) as a substrate. The second screening was conducted by ELISA using the cell lysates of chick embryonic fibroblast (CEF) cell lines that were transfected by vaccinia virus vector containing the gene either of SARS-CoV spike (S) or nucleocapsid (N) proteins.

Recombinant virus proteins: Genomic RNA was extracted from SARS-CoV strain HKU39849 and reverse transcribed to cDNA. The corresponding open reading frames (ORF) to E, M, N and S were amplified by PCR and cloned into the transfer vector, pDIsgptmH5, which also harbored *Escherichia coli* xantine-guanine phosphoribosyltransferase under the control of vaccinia virus p7.5 promoter in the cloning site of pUc/DIs (16). The recombinant clones of attenuated vaccinia virus, DIs, which harbored each ORF were obtained by homologous recombination induced in DIs-infected-, pDIsgptmH5-transfected CEF cells. The detailed protocol will be published elsewhere.

Neutralization assay: The known tissue culture infectious dose (TCID) of SARS-CoV was incubated for 1 h in the presence or absence of the purified mAbs serially diluted 10-fold, and then added to Vero E6 cell culture grown to confluence in a 96-well microtiter plate. As a control, mAbs against N protein was added to the culture. After 48 hr, cells were fixed with 10% formaldehyde and stained with crystal violet to visualize the cytopathic effect induced by the virus (17). Neutralization antibody titers were expressed as the minimum concentration of purified immunoglobulin that inhibits cytopathic effect.

Western blot: UV-inactivated purified SARS-CoV virion (0.5 μg/lane)(13) was loaded on SDS-PAGE under reduced conditions. Proteins were transferred to the PVDF membrane (Genetics, Tokyo, Japan). After blocking with BlockAce (Snow Brand Milk Products Co., Ltd., Tokyo, Japan) reagent, the membranes were reacted with the mAbs or the diluted sera (1:1000) that had been obtained from mice inoculated with UV-irradiated SARS-CoV. After washing, the membrane was reacted with peroxidase-conjugated F(ab')$_2$ fragment anti-mouse IgG (H+L) (1:20,000 Jackson Immuno Research, West Grove, Pa., USA), and the bands were visualized using chemiluminescent reagents (Amasham Biosciences, Piscataway, N.J., USA) on the X-ray film (Kodak, Rochester, N.Y., USA).

Purification and biotinylation of mAbs: Hybridomas were grown in Hybridoma-SFM medium (Invitrogen, Carlsbad, Calif., USA) supplemented with recombinant IL-6 (18) and penicillin (100 U/mL)/streptomycin (100 μg/mL). The culture supernatants were harvested, added with 1/100 volume of 1 M Tris-HCl (pH 7.4) and 1/500 volume of 10% NaN_3, and directly loaded on the Protein G-Sepharose 6B column (Amersham Biosciences). The column was washed with PBS and eluted with Glycine/HCl (pH 2.8). After measuring the OD_{280} of the fractions, protein containing fractions were pooled and added with an equal volume of saturated $(NH_4)_2SO_4$. Precipitated proteins were dissolved in PBS, dialysed against PBS and stored at −20°C. The purified antibodies were biotinylated using sulfo-NHS-LC-biotin (Pierce, Rockford, Ill., USA) according to the manufacturer's protocol.

Antigen-capture ELISA: The purified mAb for the antigen-capture was immobilized on the microplate (Immulon 2, Dynatech) by incubating 4 μg/mL antibody in 50 mM sodium bicarbonate buffer (pH 8.6) at 4°C overnight. The microplate was blocked with 1% BSA, washed with PBS-Tween, and reacted with serial dilution of UV-inactivated purified SARS-CoV for 1 h at room temperature. After washing with PBS-Tween, wells were reacted with biotinylated probing mAb (0.1 μg/mL) for 1 h at room temperature. After washing, wells were reacted with β-D-galactosidase-labeled streptavidine (Zymed) for 1 h at room temperature. After washing,

fluorescent substrate 4-methylumberyferyl-β-D-galactoside (Sigma-Aldrich, St. Louis, Mo., USA) was added and the substrate was incubated for 2 h at 37°C. The reaction was stopped by adding 0.1M Glycine-NaOH (pH 10.2) and the fluorescence (FU) of the reaction product, 4-methylumberiferron, was measured using FluoroScan (Flow Laboratories Inc., Inglewood, Calif., USA).

Histology: Formaldehyde-fixed human lung tissue that was RT-PCR positive for SARS-CoV (19) and lung from a SARS-CoV infected macaque were embedded in paraffin and sectioned using the standard method. After de-paraffinization by standard method, the sections were soaked with 0.1 M citrate-buffer (pH 6.0) and autoclaved for 10 min at 121°C to inactivate viruses. Endogenous peroxidase was inactivated by 0.3% hydrogen peroxide for 30 min at room temperature. After blocking with 5% normal goat serum for 10 min, sections were incubated with the mAb at 4°C overnight. The bound antibody was detected by biotinylated anti-mouse IgG followed by peroxidase-labeled streptavidin (LSAB2 kit, DakoCytomation, Kyoto, Japan) and visualized with 0.2 mg/mL 3,3′-diaminobenzidine in 0.015% hydrogen peroxide/0.05M Tris-HCl (pH 7.6). The sections were counterstained with hematoxylin.

RESULTS

In order to establish the hybridomas that secrete specific mAbs to SARS-CoV, we immunized BALB/c mice with purified SARS-CoV whole virion fraction. The virus was inactivated by UV-irradiation to avoid a change in antigenicity presumably caused by aldehyde-fixation or detergent-solubilization. The immunization protocols used were those of the standard method in which the boost administrations were repeated twice (protocol-1) or four times (protocol-2) with 2-week intervals using FCA/FIA as an adjuvant (see Materials and Methods). Three days after the final boost, a single cell suspension was prepared from two spleens of immunized mice and fused with SP-2/O myeloma by a polyethylene-glycol method, the fused cells were then HAT-selected (15).

In the experiment with immunization protocol-1, we found that the culture supernatants from 28 of the 1,920 wells were strong-positive in ELISA testing in which the cell-lysate of SARS-CoV infected Vero E6 cells was used as a coated antigen (Table 1). As a negative control, we used uninfected Vero E6 cell-lysate as the antigen. Wells that showed a positive reaction were omitted from the count. Among the 28 wells, 19 reacted to vaccinia vector-based recombinant-S-protein and three reacted to recombinant-N-protein. These hybridomas were successfully cloned by a repeated limiting dilution method. The remaining six wells did not give rise to a significant positive signal to recombinant-S, -N or -M proteins. One anti-S mAb cross-reacted to porcine transmissible gastroenteritis virus (TGEV) and this clone was also omitted from further studies. None of these mAbs cross-reacted to mouse hepatitis virus (MHV).

The avidities of these cloned mAbs were tested by avidity-ELISA in the presence of urea. Although in the presence of 6 M urea some anti-S mAbs retained 18-35% of the original reactivity, less than 10% of the original reactivity remained in the presence of 8 M urea (Table 2). Three anti-N mAbs showed a very low avidity index in this assay system.

In a previous report that studied human IgG avidity maturation after rubella vaccination, high-avidity antibodies were defined as those that retain more than 50% of reactivity in the presence of 8 M urea (20). Although it would not be possible to directly apply this definition of polyclonal antibodies to our mAb case, the avidities of mAbs we obtained did not seem particularly high. This prompted us to attempt to obtain better mAbs with higher avidity by repeating booster immunization in anticipation of affinity maturation. After an additional two boosts, hybridomas were established by the same procedure as the first experiment. We screened 960 wells and obtained 14 wells positive for ELISA with SARS-CoV infected Vero E6 cell lysate (Table 1). Among the 14 wells, seven reacted with recombinant-S protein and none of them reacted with recombinant-N or -M proteins. These anti-S antibodies showed significantly higher avidity in the avidity ELISA (two representative clones are shown in Table 2). From the results of this avidity test, we selected five anti-S mAbs that showed the highest avidity index. None of these mAbs cross-reacted to human coronavirus, 229E (data not shown). These five anti-S and three anti-N mAbs were purified, and characterized further.

Table 1. Summary of the first hybridoma screening by ELISA

Immobilized antigen	Experiment-1[1)]	Experiment-2[2)]	Total
(Total wells assayed)	1,920	960	2,880
SARS-CoV infected Vero cell-lysate	28	14	42
Recombinant - S	19	7	26
- N	3	0	3

[1)]: Immunization protocol-1
[2)]: Immunization protocol-2

Table 2. Avidity ELISA

Clone	Epitope	Avidity Index (%)		
		4M urea	6M urea	8M urea
Experiment-1				
SKOT-7	N	1.6	1.2	1.5
SKOT-8	N	2.3	3.2	3.7
SKOT-9	N			
SKOT-3	S	45.5	18.7	1.2
SKOT-10	S	73.4	29.9	2.6
SKOT-20	S	63.8	35.4	8.8
Experiment-2				
SOAT-5	S	51.3	48.0	43.3
SOAT-13	S	77.0	62.0	48.0

All selected mAbs worked successfully in the immunofluorescent staining assay (Fig. 1). Anti-S mAbs such as SKOT-3, -10, -20, SOAT-5 and -13 stained the Golgi body and surface membrane of virus-infected cells but not of uninfected-cells. In contrast, the staining patterns of anti-N mAbs such as SKOT-7, -8 and -9 were mainly confined to the Golgi body.

All anti-N mAbs worked in immunohistochemistry of formalin-fixed, paraffin-embedded sections of both human lung from SARS patients and SARS-CoV infected macaque lung (Fig. 2). The specificity of these stainings was confirmed by the negative results for normal lungs and several specimens from pneumonia patients including cases complicated by measles, influenza type A, herpes-simplex and herpes zoster.

The mAbs that worked for immunohistochemistry, i.e.,

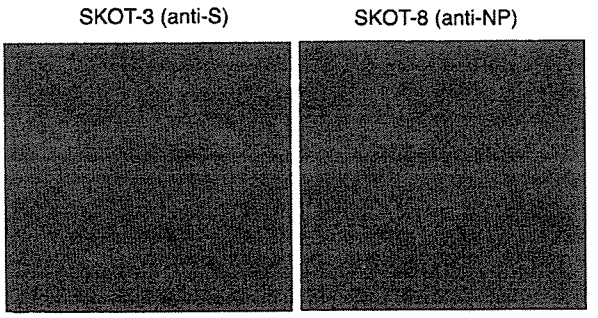

Fig. 1. Fluorescent immunostaining of SARS-CoV infected Vero E6 cells with monoclonal antibodies (mAbs). Parformaldehyde-fixed, SARS-CoV infected Vero E6 cells were permeabilized with TBS-tween and incubated with mAbs from hybridoma clones and the antibodies were detected with FITC-conjugated anti-mouse IgG. Shown are representative staining patterns with anti-S mAb, SKOT-3 (A), and anti-N mAb, SKOT-8 (B).

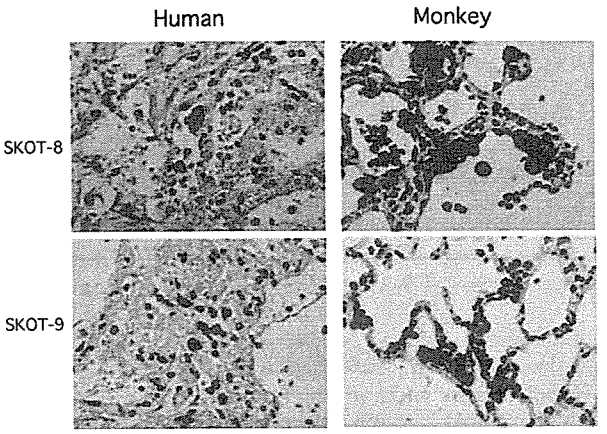

Fig. 2. Immuno-histochemistry of SARS-CoV infected human lung and macaque lung tissues with mAbs. Paraformaldehyde-fixed, paraffin-embedded sections were incubated with mAbs, and then with biotinylated anti-mouse IgG/peroxidase-labeled streptavidin complex before being visualized using DAB as a peroxidase substrate. Counter-staining with hematoxilin. Shown are human patient lung tissue (left panels) and SARS-infected macaque lung tissues (right panels), stained with anti-N mAbs (SKOT-8, SKOT-9).

SKOT-7, -8 and -9 also worked for Western-blot detection of the viral proteins (Fig. 3). Anti-N mAbs detected a band of 50 kDa that corresponds to the calculated molecular weight of SARS-CoV N-protein. In some experiments with longer exposure, a band with an apparent molecular weight of 120 kDa was also detected. None of the anti-S mAbs worked in the Western blot, suggesting that the major antigenic determinants of the S-protein are 'conformational' epitopes.

We tested the in vitro neutralizing activities of anti-S mAbs. As shown in Fig. 4, SKOT-20 neutralized in vitro SARS-CoV infection to Vero E6 cells at an antibody concentration of 1 μg/mL. Another anti-S mAb, SKOT-19, which had a low avidity value, also showed similar neutralizing activity. SKOT-10 and -3 also had neutralization activity but required higher antibody concentrations.

Lastly, we tried to construct an antigen-capture detection system for SARS-CoV by sandwich ELISA. In preliminary experiments, we tested all the combinations of two mAbs from the selected eight mAbs to obtain the highest detection sensitivity for purified SARS-CoV virion, and found that the

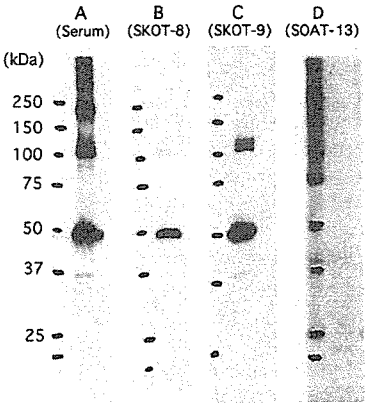

Fig. 3. Detection of virus proteins with Western blot. Purified SARS-CoV proteins (0.5 μg/lane) were electrophoresed with SDS-PAGE under reducing conditions. After blotting on the PVDF membrane, proteins were detected by incubation with mAbs, followed by incubation with peroxidase labeled-F(ab')$_2$ fragment of Donkey anti-mouse IgG. They were then visualized by chemiluminescent reaction. A: mouse serum from SARS-CoV immunized mouse; B: anti-N mAb, SKOT-8; C: anti-N mAb, SKOT-9; D: anti-S mAb, SOAT-13. The positions of molecular weight markers are shown on the left.

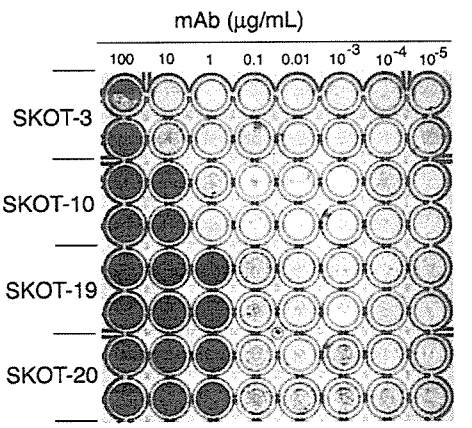

Fig. 4. In vitro neutralization assay of SARS-CoV infection with mAbs. Purified SARS-CoV fraction was diluted to 1×10^2 PFU/mL and incubated with serially-titrated purified mAbs for 1 h at 37°C. After the reaction, samples were poured into wells of a 96-well plate on which Vero E6 cells were grown to 90% confluent. After 48 h, cytotoxicities were visualized by staining the cells with crystalviolet. The results of purified anti-S antibodies (SKOT-3, -10, -19 and -20) with concentrations ranging from 100 μg/mL to 10^{-5} μg/mL are shown.

immobilization of SKOT-8 on the ELISA plate followed by the detection with biotinylated SKOT-9 gave the best result (data not shown; see Materials and Methods). In this sandwich ELISA, SARS-CoV protein was successfully detected in a concentration as low as 40 pg/mL (Fig. 5). Since the mAbs were originally raised against SARS-CoV strain HKU39849, we tested the validity of this system for other strains of SARS-CoV. As shown in Fig. 6, it was confirmed that the strains HK14T1WL, CDC00592 and Frankfurt1 were as detectable as HKU39849 using this system.

DISCUSSION

We established mAbs against SARS-CoV, which enable

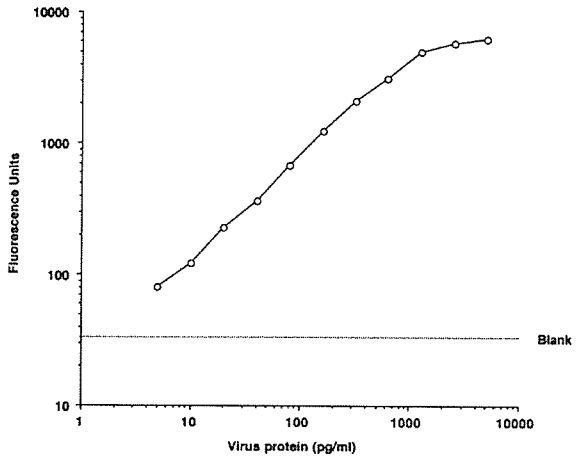

Fig. 5. Antigen-capture ELISA of SARS-CoV with mAbs. Anti-N mAb, SKOT-8, was immobilized on the surface of a 96 well plate. Serially-titrated purified SARS-CoV fractions were reacted for 1 h at room temperature and the bound virus proteins were detected by biotinylated SKOT-9 (anti-N) antibody followed by peroxydase-labeled streptavidin. They were then quantitated by chemiluminescent reaction using 4-methylumberiferril as a substrate. Abscissa: concentration of purified SARS-CoV proteins; ordinate: fluorescent unit.

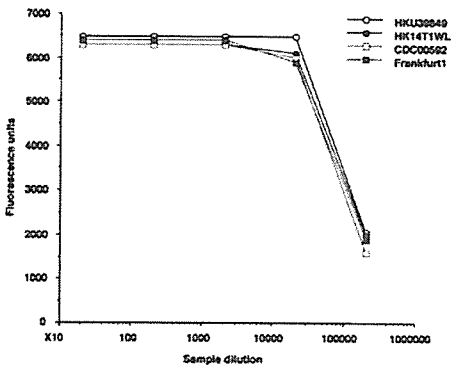

Fig. 6. Comparison of SARS-CoV strains for reactivity to the antigen capture sandwich ELISA. SARS-CoV strains, HKU39849, HK14T1WL, CDC00592 and Frankfurt1 were tested for the reactivity to the antigen-capture ELISA system as described in Fig. 5. Abscissa: sample dilution; ordinate: fluorescent units.

the detection of virus S- and N-proteins by means of immunofluorescence assay, immunohistochemistry, Western blot and antigen-capture ELISA. A summary of selected mAbs is shown in Table 3.

Among the originally selected 42 mAbs that were positive in ELISA for SARS-CoV infected Vero E6 cell lysate, 26 reacted to recombinant-S-protein and only three reacted to N-protein. We could not find hybridoma secreting mAb to M-protein or other protein components of SARS-CoV. These results suggest that S protein is the dominant target in the antibody response. We observed that none of the anti-S mAbs established worked in Western blot, suggesting that these mAbs may recognize 'conformational' epitopes. In contrast, all three anti-N mAbs worked in Western blot and immunohistochemistry, suggesting that these mAbs recognize 'linear' epitopes.

We examined whether our mAbs were applicable for immunofluorescence detection of virus-infected cells. In immunofluorescent staining of Vero E6 cells infected with SARS-CoV, anti-N mAbs stained the Golgi body and anti-S mAbs stained the Golgi body and surface membrane. This difference in localization of N- and S-proteins may reflect the common assembly process of coronaviruses (21). Further analysis is needed to clarify sensitivity and specificity in infected cells for clinical use.

During the course of outbreak of SARS-CoV in Hong Kong, it was reported that more than half the patients were not positively diagnosed by RT-PCR (8). Therefore, the diagnosis was finally confirmed by serum specimens in a convalescent-phase at a late stage of illness (8). To overcome this problem, virus shedding patterns have been extensively analyzed, with results showing that respiratory shedding of the virus increases over the first week and viral shedding in stools begins a few days after respiratory shedding (7,8). From this analysis, it is considered that a combination of stool sampling and pooled throat and nasal swab specimens could be good specimens for safe and highly sensitive SARS-CoV detection.

In general, a single diagnostic test is not conclusively reliable, because of the serious potential for false positives and negatives. Considering the limited sensitivity of RT-PCR, serological screening systems other than antibody detection are currently being examined (22,23). ELISA-based antigen captured assays are known to offer high specificity and reproducibility. Antigen-captured assays have been used in the diagnosis and monitoring of disease in cases of infection with dengue virus (24), human immunodeficient virus p24 (25) and Ebola hemorragic fever (26) and examined in hepatitis B virus and hepatitis C virus (22,23). In this context, extensive analysis in Ebola hemorragic fever suggests that the RT-PCR assay is extremely useful, but should always be utilized in combination with antigen-captured ELISA, which makes the diagnosis more reliable (26).

Table 3. Summary of selected hybridoma clones

Clone	Epitope	Class	IFA	Neutralization[1)]	Western-blot	Histology	Avidity (%)[2)]
SKOT-7	N	IgG	Golgi	-	50kDa	-	1.2
SKOT-8	N	IgG	Golgi	-	50kDa	Usable	3.2
SKOT-9	N	IgG	Golgi	-	120, 50kDa	Usable	3.8
SKOT-3	S	IgG	Golgi / cell membrane	100	-	-	18.7
SKOT-10	S	IgG	Golgi / cell membrane	10	-	-	29.9
SKOT-19	S	IgG	Golgi / cell membrane	1	ND	ND	ND
SKOT-20	S	IgG	Golgi / cell membrane	1	-	-	35.4
SOAT-5	S	IgG	Golgi / cell membrane	ND	-	-	48.0
SOAT-13	S	IgG	Golgi / cell membrane	ND	-	-	62.0

[1)]: Numbers represent minimum concentration (μg/mL) that exerts neutralization. -, no neutralization activity; ND, not determined.
[2)]: Avidity index at 6M urea (see Materials and Methods).

In the case of SARS-CoV, the assay has been recently evaluated by using mAbs and polyclonal antibodies directed against recombinant SARS-CoV nucleocapsid protein (22,23). A soluble N-protein was observed to be released from infected cells in culture, which led to the opportunity to evaluate the level in serum specimens from infected patients. N-antigen ELISA employing mAbs reproducibly detected 50% of patients on days 3 and 5 after the onset of illness, with a limitation of the detection of the recombinant protein at 50 pg/ml (22). N-antigen ELISA with use of polyclonal antibodies detected 60-50% of nasopharyngeal aspirate and fecal specimens from patients at day 3 to day 24 after the onset of illness, although the signal was relatively weak in fecal samples (22). These results suggest that antigen-captured assay could be useful for the early diagnosis of SARS-CoV infection.

We developed an antigen-capture ELISA system that detects purified SARS-CoV virion at levels as low as 40 pg/mL. The sensitivity of the system, which comprised two anti-N mAbs, seems high enough to detect virus protein in patient sera when compared to a recently reported antigen-capture ELISA system, which detects 100 pg/mL of purified recombinant N protein, successfully determined the virus protein in patient sera (22). We are now improving the sensitivity of the system and checking its applicability in the diagnosis and monitoring of SARS-CoV infection. Although none of our mAbs cross-reacted to human or other animal coronaviruses (229E, TGEV and MHV) by ELISA, it is also important to define the specificity of these mAbs by other techniques such as Western blot and immunofluorescent staining. This issue is currently under investigation.

Two anti-S mAbs, SKOT-19 and -20 demonstrated significant virus neutralizing activity. It would be interesting to address whether these mAbs interfere with the binding of the virion to its recently reported receptor, ACE2 (27). If this were the case, the humanization of these mAbs by means of either CDR-grafting or mouse-human chimeric antibody would be of interest as a possible application for the therapeutic use of these mAbs.

ACKNOWLEDGMENTS

We are grateful to Ms. Sayuri Yamaguchi for her assistance in establishing hybridomas.

This work was supported by grant from the Ministry of Health, Labour and Welfare of Japan.

REFERENCES

1. Drosten, C., Gunther, S., Preiser, W., van der Werf, S., Brodt, H. R., Becker, S., Rabenau, H., Panning, M., Kolesnikova, L., Fouchier, R. A., Berger, A., Burguiere, A. M., Cinatl, J., Eickmann, M., Escriou, N., Grywna, K., Kramme, S., Manuguerra, J. C., Muller, S., Rickerts, V., Sturmer, M., Vieth, S., Klenk, H. D., Osterhaus, A. D., Schmitz, H. and Doerr, H. W. (2003): Identification of a novel coronavirus in patients with severe acute respiratory syndrome. N. Engl. J. Med., 348, 1967-1976.
2. Ksiazek, T. G., Erdman, D., Goldsmith, C. S., Zaki, S. R., Peret, T., Emery, S., Tong, S., Urbani, C., Comer, J. A., Lim, W., Rollin, P. E., Dowell, S. F., Ling, A. E., Humphrey, C. D., Shieh, W. J., Guarner, J., Paddock, C. D., Rota, P., Fields, B., DeRisi, J., Yang, J. Y., Cox, N., Hughes, J. M., LeDuc, J. W., Bellini, W. J. and Anderson, L. J. (2003): A novel coronavirus associated with severe acute respiratory syndrome. N. Engl. J. Med., 348, 1953-1966.
3. World Health Organization (2003): Summary table of SARS cases by country, 1 November 2002 - 7 August 2003.
4. World Health Organization: WHO SARS international reference and verification laboratory network: policy and procedures in the inter-epidemic period.
5. Peiris, J. S., Chu, C. M., Cheng, V. C., Chan, K. S., Hung, I. F., Poon, L. L., Law, K. I., Tang, B. S., Hon, T. Y., Chan, C. S., Chan, K. H., Ng, J. S., Zheng, B. J., Ng, W. L., Lai, R. W., Guan, Y. and Yuen, K. Y. (2003): Clinical progression and viral load in a community outbreak of coronavirus-associated SARS pneumonia: a prospective study. Lancet, 361, 1767-1772.
6. Grant, P. R., Garson, J. A., Tedder, R. S., Chan, P. K., Tam, J. S. and Sung, J. J. (2003): Detection of SARS coronavirus in plasma by real-time RT-PCR. N. Engl. J. Med., 349, 2468-2469.
7. Cheng, P. K., Wong, D. A., Tong, L. K., Ip, S. M., Lo, A. C., Lau, C. S., Yeung, E. Y. and Lim, W. W. (2004): Viral shedding patterns of coronavirus in patients with probable severe acute respiratory syndrome. Lancet, 363, 1699-1700.
8. Chan, P. K., To, W. K., Ng, K. C., Lam, R. K., Ng, T. K., Chan, R. C., Wu, A., Yu, W. C., Lee, N., Hui, D. S., Lai, S. T., Hon, E. K., Li, C. K., Sung, J. J. and Tam, J. S. (2004): Laboratory diagnosis of SARS. Emerg. Infect. Dis., 10, 825-831.
9. Poon, L. L., Wong, O. K., Chan, K. H., Luk, W., Yuen, K. Y., Peiris, J. S. and Guan, Y. (2003): Rapid diagnosis of a coronavirus associated with severe acute respiratory syndrome (SARS). Clin. Chem., 49, 953-955.
10. Chen, W., Xu, Z., Mu, J., Yang, L., Gan, H., Mu, F., Fan, B., He, B., Huang, S., You, B., Yang, Y., Tang, X., Qiu, L., Qiu, Y., Wen, J., Fang, J. and Wang, J. (2004): Antibody response and viraemia during the course of severe acute respiratory syndrome (SARS)-associated coronavirus infection. J. Med. Microbiol., 53, 435-438.
11. Nie, Y., Wang, G., Shi, X., Zhang, H., Qiu, Y., He, Z., Wang, W., Lian, G., Yin, X., Du, L., Ren, L., Wang, J., He, X., Li, T., Deng, H. and Ding, M. (2004): Neutralizing antibodies in patients with severe acute respiratory syndrome-associated coronavirus infection. J. Infect. Dis., 190, 1119-1126.
12. Wang, W. K., Chen, S. Y., Liu, I. J., Chen, Y. C., Chen, H. L., Yang, C. F., Chen, P. J., Yeh, S. H., Kao, C. L., Huang, L. M., Hsueh, P. R., Wang, J. T., Sheng, W. H., Fang, C. T., Hung, C. C., Hsieh, S. M., Su, C. P., Chiang, W. C., Yang, J. Y., Lin, J. H., Hsieh, S. C., Hu, H. P., Chiang, Y. P., Yang, P. C. and Chang, S. C. (2004): Detection of SARS-associated coronavirus in throat wash and saliva in early diagnosis. Emerg. Infect. Dis., 10, 1213-1219.
13. Takasuka, N., Fujii, H., Takahashi, Y., Kasai, M., Morikawa, S., Itamura, S., Ishii, K., Sakaguchi, M., Ohnishi, K., Ohshima, M., Hashimoto, S., Odagiri, T., Tashiro, M., Yoshikura, H., Takemori, T. and Tsunetsugu-Yokota, Y. (2004): A subcutaneously injected UV-inactivated SARS coronavirus vaccine elicits systemic humoral immunity in mice. Int. Immunol., 16, 1423-1430.
14. Darnell, M. E., Subbarao, K., Feinstone, S. M. and Taylor, D. R. (2004): Inactivation of the coronavirus that

induces severe acute respiratory syndrome, SARS-CoV. J. Virol. Methods, 121, 85-91.
15. Kozbor, D. and Roder, J. C. (1984): In vitro stimulated lymphocytes as a source of human hybridomas. Eur. J. Immunol., 14, 23-27.
16. Ishii, K., Ueda, Y., Matsuo, K., Matsuura, Y., Kitamura, T., Kato, K., Izumi, Y., Someya, K., Ohsu, T., Honda, M. and Miyamura, T. (2002): Structural analysis of vaccinia virus DIs strain: application as a new replication-deficient viral vector. Virology, 302, 433-444.
17. Storch, G. A. (2001): Diagnostic Virology. p. 493-531. *In* Knipe, D.M., Howley, P.M., (ed.), Fields Virology. 4th ed. Vol. 1. Lippincott Williams & Wilkins, Philadelphia.
18. Karasuyama, H., Rolink, A. and Melchers, F. (1993): A complex of glycoproteins is associated with VpreB/lambda 5 surrogate light chain on the surface of mu heavy chain-negative early precursor B cell lines. J. Exp. Med., 178, 469-478.
19. Nakajima, N., Asahi-Ozaki, Y., Nagata, N., Sato, Y., Dizon, F., Paladin, F. J., Olveda, R. M., Odagiri, T., Tashiro, M. and Sata, T. (2003): SARS coronavirus-infected cells in lung detected by new in situ hybridization technique. Jpn. J. Infect. Dis., 56, 139-141.
20. Hedman, K., Hietala, J., Tiilikainen, A., Hartikainen-Sorri, A. L., Raiha, K., Suni, J., Vaananen, P. and Pietilainen, M. (1989): Maturation of immunoglobulin G avidity after rubella vaccination studied by an enzyme linked immunosorbent assay (avidity-ELISA) and by haemolysis typing. J. Med. Virol., 27, 293-298.
21. Lai, M. M. C. and Holmes, K. V. (2001): *Coronaviridae*: the viruses and their replication. *In* Knipe, D. M. and Howley, P. M. (ed.), Fields Virology. 4th ed. Vol. 1. Lippincott Williams & Wilkins, Philadelphia.
22. Che, X. Y., Qiu, L. W., Pan, Y. X., Wen, K., Hao, W., Zhang, L. Y., Wang, Y. D., Liao, Z. Y., Hua, X., Cheng, V. C. and Yuen, K. Y. (2004): Sensitive and specific monoclonal antibody-based capture enzyme immunoassay for detection of nucleocapsid antigen in sera from patients with severe acute respiratory syndrome. J. Clin. Microbiol., 42, 2629-2635.
23. Lau, S. K., Woo, P. C., Wong, B. H., Tsoi, H. W., Woo, G. K., Poon, R. W., Chan, K. H., Wei, W. I., Peiris, J. S. and Yuen, K. Y. (2004): Detection of severe acute respiratory syndrome (SARS) coronavirus nucleocapsid protein in SARS patients by enzyme-linked immunosorbent assay. J. Clin. Microbiol., 42, 2884-2889.
24. Young, P. R., Hilditch, P. A., Bletchly, C. and Halloran, W. (2000): An antigen capture enzyme-linked immunosorbent assay reveals high levels of the dengue virus protein NS1 in the sera of infected patients. J. Clin. Microbiol., 38, 1053-1057.
25. Sutthent, R., Gaudart, N., Chokpaibulkit, K., Tanliang, N., Kanoksinsombath, C. and Chaisilwatana, P. (2003): p24 Antigen detection assay modified with a booster step for diagnosis and monitoring of human immunodeficiency virus type 1 infection. J. Clin. Microbiol., 41, 1016-1022.
26. Towner, J. S., Rollin, P. E., Bausch, D. G., Sanchez, A., Crary, S. M., Vincent, M., Lee, W. F., Spiropoulou, C. F., Ksiazek, T. G., Lukwiya, M., Kaducu, F., Downing, R. and Nichol, S. T. (2004): Rapid diagnosis of Ebola hemorrhagic fever by reverse transcription-PCR in an outbreak setting and assessment of patient viral load as a predictor of outcome. J. Virol., 78, 4330-4341.
27. Li, W., Moore, M. J., Vasilieva, N., Sui, J., Wong, S. K., Berne, M. A., Somasundaran, M., Sullivan, J. L., Luzuriaga, K., Greenough, T. C., Choe, H. and Farzan, M. (2003): Angiotensin-converting enzyme 2 is a functional receptor for the SARS coronavirus. Nature, 426, 450-454.

Nucleic Acids Research, 2005, Vol. 33, No. 6 **e65**
doi:10.1093/nar/gni064

Species-independent detection of RNA virus by representational difference analysis using non-ribosomal hexanucleotides for reverse transcription

Daiji Endoh*, Tetsuya Mizutani[1], Rikio Kirisawa[2], Yoshiyuki Maki[3], Hidetoshi Saito[3], Yasuhiro Kon[4], Shigeru Morikawa[1] and Masanobu Hayashi

Laboratory of Veterinary Radiology, School of Veterinary Medicine, Rakuno Gakuen University, Ebetsu 069-8501, Japan, [1]Special Pathogens Laboratory, Department of Virology 1, National Institute of Infectious Diseases, Musashimurayama 208-0011, Japan, [2]Laboratory of Veterinary Microbiology, School of Veterinary Medicine, Rakuno Gakuen University, Ebetsu 069-8501, Japan, [3]Genosys Division, Sigma-Aldrich Japan, Ishikari 061-3241, Japan and [4]Laboratory of Anatomy, Graduate School of Veterinary Medicine, Hokkaido University, Sapporo 060-0818, Japan

Received December 10, 2004; Revised February 26, 2005; Accepted March 18, 2005

ABSTRACT

A method for the isolation of genomic fragments of RNA virus based on cDNA representational difference analysis (cDNA RDA) was developed. cDNA RDA has been applied for the subtraction of poly(A)$^+$ RNAs but not for poly(A)$^-$ RNAs, such as RNA virus genomes, owing to the vast quantity of ribosomal RNAs. We constructed primers for inefficient reverse transcription of ribosomal sequences based on the distribution analysis of hexanucleotide patterns in ribosomal RNA. The analysis revealed that distributions of hexanucleotide patterns in ribosomal RNA and virus genome were different. We constructed 96 hexanucleotides (non-ribosomal hexanucleotides) and used them as mixed primers for reverse transcription of cDNA RDA. A synchronous analysis of hexanucleotide patterns in known viral sequences showed that all the known genomic-size viral sequences include non-ribosomal hexanucleotides. In a model experiment, when non-ribosomal hexanucleotides were used as primers, *in vitro* transcribed plasmid RNA was efficiently reverse transcribed when compared with ribosomal RNA of rat cells. Using non-ribosomal primers, the cDNA fragments of severe acute respiratory syndrome coronavirus and bovine parainfluenza virus 3 were efficiently amplified by subtracting the cDNA amplicons derived from uninfected cells from those that were derived from virus-infected cells. The results suggest that cDNA RDA with non-ribosomal primers can be used for species-independent detection of viruses, including new viruses.

INTRODUCTION

Identifying the causative agent of an infectious disease is the cornerstone for its eventual control. For example, the outbreak of severe acute respiratory syndrome (SARS) was controlled after the identification of the causative agent coronavirus (SARS-CoV) (1). Developments in molecular biological approaches in recent years have led to the identification of many unknown pathogens. Once a fragment from the agent's genome has been isolated and sequenced, standard genomic walking techniques are used to extend the known sequence, and computer homology searches can then be used to identify the likely phylogenetic relationship of the agent with other known organisms (2). Additionally, sequences of some viruses, such as SARS-CoV, have altered during transmission, and this may prevent the detection of the virus by a PCR method (3,4). Thus, a detection method that is not based on the known sequence is essentially required as an alternative method to the normal PCR method.

Representational difference analysis (RDA) is one of the most reliable methods for identifying new agents since it does not require prior knowledge of the agent's class (5). The technique is based on PCR enrichment of DNA fragments that are present in agent-infected cells but absent in normal cells. Using RDA, Chang *et al.* (6) isolated two DNA fragments

*To whom correspondence should be addressed. Tel: +81 11 388 4847; Fax: +81 11 387 5890; Email: dendoh@rakuno.ac.jp